

Appendix A

Mandelstam Variables

Take a $(p_1, p_2) \rightarrow (p_3, p_4)$ scattering processes, where $p_{1,2}$ and $p_{3,4}$ are, respectively, the 4-momentum of the incoming and outcoming particles. Because of 4-momentum conservation,

$$p_1 + p_2 = p_3 + p_4 \quad (\text{A.1})$$

If the invariant mass of i particle is m_i , then

$$p_i^2 = (p_{i0}, p_{i1}, p_{i2}, p_{i3})^2 = p_{i0}^2 - p_{i1}^2 - p_{i2}^2 - p_{i3}^2 = m_i^2 \quad (\text{A.2})$$

So, we have, for the four cases ($E_i, i = 1, 2, 3, 4$),

$$E_i^2 = p_i'^2 + m_i^2 \quad (\text{A.3})$$

Without loss of generality, for a scattering process in the center of mass (CM) frame, we can take

$$p_1 = (E_1, 0, 0, p_1') \quad (\text{A.4})$$

$$p_2 = (E_2, 0, 0, -p_1') \quad (\text{A.5})$$

$$p_3 = (E_3, 0, p_3' \sin \theta, p_3' \cos \theta) \quad (\text{A.6})$$

$$p_4 = (E_4, 0, -p_3' \sin \theta, -p_3' \cos \theta) \quad (\text{A.7})$$

where θ is the angle between particles 1 and 3 in the CM. The Mandelstam variables¹ s , t and u are defined as

$$s = (p_1 + p_2)^2 = (p_3 + p_4)^2 \quad (\text{A.8})$$

$$t = (p_1 - p_3)^2 = (p_2 - p_4)^2 \quad (\text{A.9})$$

$$u = (p_1 - p_4)^2 = (p_2 - p_3)^2 \quad (\text{A.10})$$

¹ See, for example, Ref. [1].

So, using momentum conservation (A.1) and rel. (A.2),

$$s + t + u = p_1^2 + p_2^2 + p_3^2 + p_4^2 = m_1^2 + m_2^2 + m_3^2 + m_4^2 \quad (\text{A.11})$$

With Eq. (A.3) and Eqs. (A.4)–(A.10),

$$p_{1,3}^{\prime 2} = \frac{(s - m_{1,3}^2 - m_{2,4}^2)^2 - 4m_{1,3}^2 m_{2,4}^2}{4s} \quad (\text{A.12a})$$

$$\begin{aligned} t &= (p_1 - p_3)^2 = (E_1 - E_3)^2 - p_3'^2 - p_1'^2 + 2p_1' p_3' \cos \theta \\ &= m_1^2 + m_3^2 - 2\sqrt{m_1^2 + p_1'^2} \sqrt{m_3^2 + p_3'^2} + 2p_1' p_3' \cos \theta \end{aligned} \quad (\text{A.12b})$$

$$u = m_1^2 + m_2^2 + m_3^2 + m_4^2 - s - t \quad (\text{A.12c})$$

Now, if we take the particular case $m_1 = m_2$ and $m_3 = m_4$ (both incoming and outgoing particle pairs have the same mass), these last expressions simplify to

$$p_{1,3}^{\prime 2} = \frac{s}{4} - m_{1,3}^2 \rightarrow p_{1,3}' = \frac{\sqrt{s}}{2} \sqrt{1 - \frac{4m_{1,3}^2}{s}} \quad (\text{A.13})$$

$$t = m_1^2 + m_3^2 - \frac{s}{2} \left(1 - \sqrt{1 - \frac{4m_1^2}{s}} \sqrt{1 - \frac{4m_3^2}{s}} \cos \theta \right) \quad (\text{A.14})$$

The scattering angle θ can be expressed as

$$\cos \theta = \frac{1}{\sqrt{1 - \frac{4m_1^2}{s}} \sqrt{1 - \frac{4m_3^2}{s}}} \left(1 + \frac{2(t - m_1^2 - m_3^2)}{s} \right) \quad (\text{A.15})$$

Finally, if all the masses are zero,

$$t = -\frac{s}{2} (1 - \cos \theta) \quad (\text{A.16})$$

$$u = -\frac{s}{2} (1 + \cos \theta) \quad (\text{A.17})$$

$$\cos \theta = 1 + \frac{2t}{s} \quad (\text{A.18})$$

Reference

- 1 M.E. Peskin, D.V. Schroeder, *An Introduction to Quantum Field Theory*; 1995 ed. (Westview, Boulder, CO, 1995)

Appendix B

Spinor Computation

B.1 $t\bar{t}$ in the Final State

The goal of this appendix is to prove Eq. 3.104,

$$\bar{u}^+(p_1) v^+(p_2) = +\sqrt{s - 4M_t^2} = +\sqrt{s} + \mathcal{O}\left(\frac{M_t^2}{s}\right). \quad (\text{B.1a})$$

$$\bar{u}^+(p_1) v^-(p_1) = 0. \quad (\text{B.1b})$$

$$\bar{u}^-(p_1) v^+(p_2) = 0. \quad (\text{B.1c})$$

$$\bar{u}^-(p_1) v^-(p_2) = -\sqrt{s - 4M_t^2} = -\sqrt{s} + \mathcal{O}\left(\frac{M_t^2}{s}\right), \quad (\text{B.1d})$$

where u and v are the spinors associated with the $t\bar{t}$ final state in $\omega\omega \rightarrow t\bar{t}$ and $hh \rightarrow t\bar{t}$ processes. These spinors are defined as²

$$u(p_1, \xi, \lambda_1) = \begin{pmatrix} \sqrt{(p_1 \cdot \sigma)} \xi \\ \sqrt{(p_1 \cdot \bar{\sigma})} \xi \end{pmatrix}, \quad v(p_2, \eta, \lambda_2) = \begin{pmatrix} \sqrt{(p_2 \cdot \sigma)} \eta \\ -\sqrt{(p_2 \cdot \bar{\sigma})} \eta \end{pmatrix} \quad (\text{B.2a})$$

where u and v are, respectively, a particle (the top quark, t) and antiparticle (the anti-top quark, \bar{t}); p , the 4-momentum of the final state particles referred to the center of mass frame; and ξ, η , the corresponding 2-component spinors. These spinors are normalized (see Refs. [1–3]) by

$$\xi^\dagger \xi = \eta^\dagger \eta = 1. \quad (\text{B.3})$$

Note that the square roots of Eq. B.2 are defined for complex 2×2 matrices. The square root of a matricial operator, in its diagonal form, is defined as the diagonal matrix of the square root of its eigenvalues. Note that the positive determination is

²See, for instance, Refs. [1–3].

used here (at the end, the eigenvalues will be real and positive). If the operator is not in a diagonal form, then it will be rotated in order to compute the square root matrix. Note that, in general, this definition of a square root does not verify the property $\sqrt{AB} = \sqrt{A}\sqrt{B}$, only applicable when A and B have a common eigenbasis.

Now, let us use the Weyl basis (see Refs. [1–3]), where

$$\gamma^0 = \begin{pmatrix} 0 & \mathbb{1}_{2 \times 2} \\ \mathbb{1}_{2 \times 2} & 0 \end{pmatrix} \quad (\text{B.4a})$$

$$\sigma \equiv (\mathbb{1}_{2 \times 2}, \hat{\sigma}) \quad (\text{B.4b})$$

$$\bar{\sigma} \equiv (\mathbb{1}_{2 \times 2}, -\hat{\sigma}) \quad (\text{B.4c})$$

$$\hat{\sigma} \equiv (\sigma_1, \sigma_2, \sigma_3), \quad (\text{B.4d})$$

σ_i ($i = 1, 2, 3$) being the Pauli matrices. Furthermore, since we are in the center of mass frame,

$$p_1 = (E, \vec{p}), \quad p_2 = (E, -\vec{p}) \quad (\text{B.5a})$$

$$\vec{p} = p(\sin \theta \cos \phi, \sin \theta \sin \phi, \cos \theta). \quad (\text{B.5b})$$

We could have taken $\theta = \phi = 0$, without loss of generality. However, let us keep the complete computation, which will be illustrative for the more general case of Sect. B.2. Note that, because of Eqs. B.4 and B.5,

$$(p_1 \cdot \sigma) = \begin{pmatrix} E - p \cos \theta & -pe^{-i\phi} \sin \theta \\ -pe^{i\phi} \sin \theta & E + p \cos \theta \end{pmatrix}, \quad (p_1 \cdot \bar{\sigma}) = \begin{pmatrix} E + p \cos \theta & -pe^{-i\phi} \sin \theta \\ -pe^{i\phi} \sin \theta & E - p \cos \theta \end{pmatrix}. \quad (\text{B.6})$$

Note that both $(p_1 \cdot \sigma)$ and $(p_1 \cdot \bar{\sigma})$ are 2×2 hermitian matrices, so that they are diagonalizable by an orthonormal basis of eigenvectors with real eigenvalues. Indeed, the eigenvalues of $(p_1 \cdot \sigma)$ are $E - p$ and $E + p$, with the corresponding eigenvectors v_λ ,

$$v_{E-p} = \begin{pmatrix} \cos \frac{\theta}{2} \\ e^{i\phi} \sin \frac{\theta}{2} \end{pmatrix}, \quad v_{E+p} = \begin{pmatrix} e^{-i\phi} \sin \frac{\theta}{2} \\ -\cos \frac{\theta}{2} \end{pmatrix}. \quad (\text{B.7})$$

For $(p_1 \cdot \bar{\sigma})$, the eigenvalues and eigenvectors (v'_λ) are obtained by swapping $p \rightarrow -p$ on those for $(p_1 \cdot \sigma)$,

$$v'_{E+p} = v_{E-p} = \begin{pmatrix} \cos \frac{\theta}{2} \\ e^{i\phi} \sin \frac{\theta}{2} \end{pmatrix}, \quad v'_{E-p} = v_{E+p} = \begin{pmatrix} e^{-i\phi} \sin \frac{\theta}{2} \\ -\cos \frac{\theta}{2} \end{pmatrix}. \quad (\text{B.8})$$

And, finally, the definition of \bar{k} is $\bar{k} \equiv k^\dagger \gamma^0$ for any 4-vector k , where the matrix γ^0 is defined in Eq. B.4a. Hence, the expression we are trying to compute, $\bar{u}_1^\lambda v_2^\lambda$ (Eq. B.1), turns into

$$\bar{u}_1^\lambda v_2^\lambda \equiv (u^{\lambda_1})^\dagger \gamma^0 v^{\lambda_2} = \left(\xi^\dagger \sqrt{(p_1 \cdot \sigma)}^\dagger, \xi^\dagger \sqrt{(p_1 \cdot \bar{\sigma})}^\dagger \right) \cdot \gamma^0 \cdot \begin{pmatrix} \sqrt{(p_2 \cdot \sigma)} \eta \\ -\sqrt{(p_2 \cdot \bar{\sigma})} \eta \end{pmatrix} \quad (\text{B.9})$$

Now, taking into account the definitions of Eqs. B.4, B.5, and B.9 becomes

$$\bar{u}_1^\lambda v_2^\lambda = \xi^\dagger \left[-\sqrt{(p_1 \cdot \sigma)}^\dagger \sqrt{(p_1 \cdot \sigma)} + \sqrt{(p_1 \cdot \bar{\sigma})}^\dagger \sqrt{(p_1 \cdot \bar{\sigma})} \right] \eta. \quad (\text{B.10})$$

Now, consider that both $(p_1 \cdot \sigma)$ and $(p_1 \cdot \bar{\sigma})$ are hermitian matrices with positive eigenvalues ($\sqrt{E-p}$ and $\sqrt{E+p}$). Then, the matricial square roots will also be hermitian, so that Eq. B.10 reduces to

$$\bar{u}^{\lambda_1} v^{\lambda_2} = \xi^\dagger [-(p_1 \cdot \sigma) + (p_1 \cdot \bar{\sigma})] \eta = 2p[\xi^\dagger (\hat{p} \cdot \hat{\sigma}) \eta], \quad (\text{B.11})$$

where $\vec{p} \equiv p\hat{p}$ is a 3-vector. Now, because the helicity operator Σ for a particle with 3-momenta \vec{p} is

$$\hat{h} = \hat{p} \cdot \hat{\sigma}. \quad (\text{B.12})$$

Let us introduce the notation η^{λ_i} and ξ^{λ_i} for the spinors ($i = 1, 2$), where the $\lambda_i = \pm$ superindex stands for the helicity state $h = \pm 1$ of the particle i . Because changing particle by anti-particle changes the helicity sign, as does changing \vec{p} by $-\vec{p}$, Eq. B.11 turns into

$$\bar{u}^{\lambda_1} v^{\lambda_2} = 2ph^{\lambda_2} (\xi^{\lambda_1})^\dagger \xi^{\lambda_2}. \quad (\text{B.13})$$

Finally, according to the orthonormality of helicity states (Eq. B.3 and $\eta^\pm \cdot \eta^\mp = \xi^\pm \cdot \xi^\mp = 0$), and to the definition of s Mandelstam variable (Eq. A.8), we recover Eq. 3.104 (quoted in Eq. B.1),

$$\bar{u}^{\lambda_1} v^{\lambda_2} = 2ph^{\lambda_1} \delta_{\lambda_1, \lambda_2} = 2h^{\lambda_1} \sqrt{E^2 - M_t^2} \delta_{\lambda_1, \lambda_2} = h^{\lambda_1} \sqrt{s - 4M_t^2} \delta_{\lambda_1, \lambda_2}, \quad (\text{B.14})$$

where $h^\pm = \pm 1$.

B.2 Analysis of the Spinors of the $t\bar{t} \rightarrow t\bar{t}$ Process

The goal of this appendix is the computation of the spinor chains which appear on the $t\bar{t} \rightarrow t\bar{t}$ scattering amplitude in Eq. 3.118. First of us, let us define the notation

$$[t(p_1, u_1, \xi_1, \lambda_1), \bar{t}(p_2, v_2, \eta_2, \lambda_2)] \rightarrow [t(p_3, u_3, \xi_3, \lambda_3), \bar{t}(p_4, v_4, \eta_4, \lambda_4)]. \quad (\text{B.15})$$

Here, p_i ($i = 1, 2, 3, 4$) stands for the 4-momentum of the initial and final state particles; u_i ($i = 1, 3$) and v_i ($i = 2, 4$), for the spinors of the top quarks and antiquarks, respectively; ξ_i ($i = 1, 3$) and η_i ($i = 2, 4$), for the polarization vectors of the quarks and antiquarks; and λ_i ($i = 1, 2, 3, 4$), for the helicities of the particles.

Now, in the center of mass frame, and taking into account that all the particles and antiparticles have the same mass (the top quark one, M_t) and the 4-momenta conservation ($p_1 + p_2 = p_3 + p_4$), the 4-momenta may be chosen as

$$p_1 = (E, 0, 0, p) \quad p_2 = (E, 0, 0, -p) \quad (\text{B.16a})$$

$$p_3 = (E, \vec{p}) \quad p_4 = (E, -\vec{p}), \quad (\text{B.16b})$$

where \vec{p} is defined in spherical coordinates,

$$\vec{p} = p(\sin \theta \cos \phi, \sin \theta \sin \phi, \cos \theta). \quad (\text{B.16c})$$

As in the case of the previous Appendix B.1, we will work in the Weyl basis. See Refs. [1–3] for an introduction to Dirac spinors in such a basis. The spinors are defined as

$$u(p_i, \xi, \lambda) = \begin{pmatrix} \sqrt{(p_i \cdot \sigma)} \xi \\ \sqrt{(p_i \cdot \bar{\sigma})} \xi \end{pmatrix}, \quad v(p_i, \eta, \lambda) = \begin{pmatrix} \sqrt{(p_i \cdot \sigma)} \eta \\ -\sqrt{(p_i \cdot \bar{\sigma})} \eta \end{pmatrix} \quad (\text{B.17a})$$

$$\gamma^0 = \begin{pmatrix} 0 & \mathbb{1}_{2 \times 2} \\ \mathbb{1}_{2 \times 2} & 0 \end{pmatrix}, \quad \gamma^5 = \begin{pmatrix} -\mathbb{1}_{2 \times 2} & 0 \\ 0 & \mathbb{1}_{2 \times 2} \end{pmatrix} \quad (\text{B.17b})$$

$$u_i^{\lambda_i} = \begin{pmatrix} \sqrt{p_i \cdot \sigma} \xi^{\lambda_i} \\ \sqrt{p_i \cdot \bar{\sigma}} \xi^{\lambda_i} \end{pmatrix}, \quad v_j^{\lambda_j} = \begin{pmatrix} \sqrt{p_j \cdot \sigma} \eta^{\lambda_j} \\ -\sqrt{p_j \cdot \bar{\sigma}} \eta^{\lambda_j} \end{pmatrix}, \quad i = 1, 3, j = 2, 4 \quad (\text{B.17c})$$

$$\sigma = (\mathbb{1}_{2 \times 2}, \hat{\sigma}), \quad \bar{\sigma} = (\mathbb{1}_{2 \times 2}, -\hat{\sigma}), \quad \hat{\sigma} = (\sigma_1, \sigma_2, \sigma_3), \quad (\text{B.17d})$$

and $\bar{k} \equiv k^\dagger \gamma^0$ for any 4-vector k . Note that σ_i ($i = 1, 2, 3$) are the Pauli matrices,³ and that we are making the same definitions in Eq. B.17d that in Eq. B.4 in the previous Appendix B.1.

Now, Eq. B.12 defines the helicity operator for particles,

$$\hat{h}_i = \hat{p}_i \cdot \hat{\sigma} = \begin{pmatrix} \cos \theta_i & e^{-i\phi_i} \sin \theta_i \\ e^{i\phi_i} \sin \theta_i & -\cos \theta_i \end{pmatrix}, \quad i = 1, 3 \quad (\text{B.18})$$

where $\vec{p} = p\hat{p}$. Note that, by definition (Eq. B.16), $\theta_1 = \phi_1 = 0$ for the p_1 initial state 4-momentum. For antiparticles, there is a change of sign,

$$\hat{h}'_i = -\hat{p}_i \cdot \hat{\sigma}, \quad i = 2, 4. \quad (\text{B.19})$$

The polarization vectors will be the corresponding eigenvectors of operators B.18 and B.19, so that

³Defined, for instance, in Refs. [1–3].

$$\xi_i^+ = [\cos(\theta/2), e^{i\phi} \sin(\theta/2)] \quad \xi_i^- = [e^{-i\phi} \sin(\theta/2), -\cos(\theta/2)] \quad (\text{B.20a})$$

$$\eta_i^+ = [\sin(\theta/2), -e^{i\phi} \cos(\theta/2)] \quad \eta_i^- = [e^{-i\phi} \cos(\theta/2), \sin(\theta/2)] \quad (\text{B.20b})$$

These definitions verify the closure relations

$$(\xi_i^{\lambda_1})^\dagger \cdot \xi_i^{\lambda_2} = \delta_{\lambda_1, \lambda_2} \quad (\text{B.21a})$$

$$(\eta_i^{\lambda_1})^\dagger \cdot \eta_i^{\lambda_2} = \delta_{\lambda_1, \lambda_2} \quad (\text{B.21b})$$

$$(\xi_i^{\lambda_1})^\dagger \cdot \eta_i^{\lambda_1} = 0 \quad \forall \lambda_1 = \pm \quad (\text{B.21c})$$

Indeed, $\eta_i^\pm = \xi_i^\pm |_{\vec{p} \rightarrow -\vec{p}}$. Note also that ξ_i^\pm and η_i^\pm are eigenvectors of the corresponding helicity operator, $\hat{h}_i^\pm \xi_i^\pm = (\pm 1) \xi_i^\pm$ ($i = 1, 3$), $\hat{h}_i' \eta_i^\pm = (\pm 1) \eta_i^\pm$ ($i = 2, 4$). Note that the correct 3-momentum \vec{p} should enter the definitions of \hat{h} , \hat{h}' (Eq. B.18 and B.19).

Now, consider that, according to Eq. B.8 a generic $(p_i \cdot \sigma)$ operator will be hermitian and diagonalizable by

$$(p_i \cdot \sigma) = \begin{pmatrix} \cos \frac{\theta_i}{2} & e^{-i\phi_i} \sin \frac{\theta_i}{2} \\ e^{i\phi_i} \sin \frac{\theta_i}{2} & -\cos \frac{\theta_i}{2} \end{pmatrix} \cdot \begin{pmatrix} E_i - p_i & 0 \\ 0 & E_i + p_i \end{pmatrix} \cdot \begin{pmatrix} \cos \frac{\theta_i}{2} & e^{-i\phi_i} \sin \frac{\theta_i}{2} \\ e^{i\phi_i} \sin \frac{\theta_i}{2} & -\cos \frac{\theta_i}{2} \end{pmatrix}^\dagger. \quad (\text{B.22})$$

The corresponding square root will be defined by

$$\begin{aligned} \sqrt{(p_i \cdot \sigma)} &= \\ &= \begin{pmatrix} \cos \frac{\theta_i}{2} & e^{-i\phi_i} \sin \frac{\theta_i}{2} \\ e^{i\phi_i} \sin \frac{\theta_i}{2} & -\cos \frac{\theta_i}{2} \end{pmatrix} \cdot \begin{pmatrix} \sqrt{E_i - p_i} & 0 \\ 0 & \sqrt{E_i + p_i} \end{pmatrix} \cdot \begin{pmatrix} \cos \frac{\theta_i}{2} & e^{-i\phi_i} \sin \frac{\theta_i}{2} \\ e^{i\phi_i} \sin \frac{\theta_i}{2} & -\cos \frac{\theta_i}{2} \end{pmatrix}^\dagger. \end{aligned} \quad (\text{B.23})$$

If, on the other hand, we considered $(p_i \cdot \bar{\sigma})$ and $\sqrt{(p_i \cdot \bar{\sigma})}$, then we would recover the diagonalization just by swapping $[(E_i - p_i) \leftrightarrow (E_i + p_i)]$ on the diagonal matrices of Eqs. B.22 and B.23 (see the discussion after Eq. B.7).

Note also that, if $i = 1$ in Eqs. B.22 and B.23, that is, if we had $\theta_1 = 0$ and $\phi_1 = 0$, then the change of basis matrix which diagonalized $(p_1 \cdot \sigma)$ and $(p_1 \cdot \bar{\sigma})$ would be the identity. That is, $(p_1 \cdot \sigma)$ and $(p_1 \cdot \bar{\sigma})$ would be diagonal matrices. Furthermore, note that, because of the definitions of the 4-momenta (Eq. B.16) and the $(\sigma, \bar{\sigma})$ matrices (Eq. B.17), we have that

$$(p_i \cdot \sigma) = (p_{i+1} \cdot \bar{\sigma}), \quad (p_i \cdot \bar{\sigma}) = (p_{i+1} \cdot \sigma), \quad i = 1, 3 \quad (\text{B.24})$$

Now, taking into account all the definitions introduced in this section until now, we can evaluate the fermion chains of Eq. 3.118 for the $\mathcal{S}(t\bar{t} \rightarrow t\bar{t})$. This, indeed, is the goal of the present section.

Table B.1 Fermion bilinears which appear in Eq. 3.118, and whose computation is the goal of this Appendix B.2. Note that, as expected in the previous Appendix B.1, $\bar{u}_1^\lambda(p_1)v_2^{\lambda'}(p_2) = \bar{u}_3^\lambda(p_3)v_4^{\lambda'}(p_4) = 2ph^\lambda\delta_{\lambda,\lambda'}$.

$\lambda\lambda'$	++	+-	-+	-
$\bar{u}_1^\lambda(p_1)v_2^{\lambda'}(p_2)$	$2p$	0	0	$-2p$
$\bar{u}_3^\lambda(p_3)v_4^{\lambda'}(p_4)$	$2p$	0	0	$-2p$
$\bar{v}_2^\lambda(p_2)u_1^{\lambda'}(p_1)$	$2p$	0	0	$-2p$
$\bar{u}_3^\lambda(p_3)u_1^{\lambda'}(p_1)$	$2m \cos \frac{\theta}{2}$	$2e^{-i\phi}E \sin \frac{\theta}{2}$	$-2e^{i\phi}E \sin \frac{\theta}{2}$	$2m \cos \frac{\theta}{2}$
$\bar{v}_2^\lambda(p_2)v_4^{\lambda'}(p_4)$	$-2m \cos \frac{\theta}{2}$	$2e^{-i\phi}E \sin \frac{\theta}{2}$	$-2e^{i\phi}E \sin \frac{\theta}{2}$	$-2m \cos \frac{\theta}{2}$
$\bar{u}_3^\lambda(p_3)\gamma^5 v_4^{\lambda'}(p_4)$	$-2E$	0	0	$-2E$
$\bar{v}_2^\lambda(p_2)\gamma^5 u_1^{\lambda'}(p_1)$	$2E$	0	0	$2E$
$\bar{u}_3^\lambda(p_3)\gamma^5 u_1^{\lambda'}(p_1)$	0	$-2e^{-i\phi}p \sin \frac{\theta}{2}$	$-2e^{i\phi}p \sin \frac{\theta}{2}$	0
$\bar{v}_2^\lambda(p_2)\gamma^5 v_4^{\lambda'}(p_4)$	0	$2e^{-i\phi}p \sin \frac{\theta}{2}$	$2e^{i\phi}p \sin \frac{\theta}{2}$	0

To sum up, our definitions are: Eq. B.16, for the momenta; Eq. B.17, for the spinors and γ -matrices⁴; Eq. B.20, for the helicity vectors, which correspond to the different polarizations; and Eq. B.23 for the definition of the square roots of matrices which appear in Eq. B.17. The results can be found on Table B.1

References

- 1 M.E. Peskin, D.V. Schroeder, *An Introduction to Quantum Field Theory*; 1995 ed. (Westview, Boulder, CO, 1995)
- 2 J.F. Donoghue, E. Golowich, B.R. Holstein, *Dynamics of the Standard Model*. Cambridge Monographs on Particle Physics, Nuclear Physics, and Cosmology (Cambridge University Press, Cambridge, 1992)
- 3 P. Ramond, *Field Theory: A Modern Primer*. Frontiers in Physics (Westview Press, New York, 1997)

⁴Remember that $\bar{k} \equiv k^\dagger \gamma^0$ for any 4-vector k .

Appendix C

Dimensional Regularization and Passarino–Veltman Functions

For computing the amplitudes at NLO, the set of programs FeynRules [1], FeynArts [2] and FormCalc [3, 4] has been used. These programs take as input a Lagrangian and a wanted scattering process, and give as output its matrix element. FeynRules could also give a so-called UFO file [5], which is useful to use as input for Monte Carlo (MC) simulation programs.

The multi-loop computation requires to integrate over all the possible 4-momenta (including off-shellness) of the particles inside the loop. For 1-loop computation, there is only one 4-momentum which has to be integrated. This integration can lead both to ultraviolet (UV, limit $k \rightarrow \infty$) and infrared (IR, limit $k \rightarrow 0$) singularities.

To deal with the UV divergences, FormCalc uses the *dimensional regularization* and expresses the total amplitudes in terms of the so-called *Passarino–Veltman functions*. FormCalc defines them in the following way:

$$A_0^{(r)}(m) = \frac{\mu^{4-D}}{i\pi^2} \int \frac{d^D k}{(2\pi)^{D-4}} \frac{1}{(k^2 - m^2 + i\varepsilon)^r}, \quad r \geq 1 \quad (\text{C.1a})$$

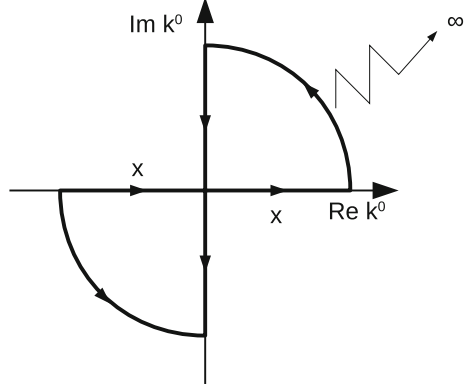
$$B_0(p^2; m_1, m_2) = \frac{(2\pi\mu)^{4-D}}{i\pi^2} \int \frac{d^D k}{[k^2 - m_1^2][(k+p)^2 - m_2^2]} \quad (\text{C.1b})$$

$$\begin{aligned} C_0(p_1^2, p_2^2, p_3^2; m_1, m_2, m_3) = \\ = \frac{1}{i\pi^2} \int \frac{d^4 k}{[k^2 - m_1^2][(k+p_1)^2 - m_2^2][(k+p_1+p_2)^2 - m_3^2]} \end{aligned} \quad (\text{C.1c})$$

$$\begin{aligned} D_0(p_1^2, p_2^2, p_3^2, p_4^2; (p_2+p_3)^2, (p_1+p_2)^2; m_1, m_2, m_3, m_4) = \\ = \frac{1}{i\pi^2} \int \frac{d^4 k}{[k^2 - m_1^2][(k+p_1)^2 - m_2^2][(k+p_1+p_2)^2 - m_3^2][(k+p_1+p_2+p_3)^2 - m_4^2]} \end{aligned} \quad (\text{C.1d})$$

Usually, Refs. [6, 7] are credited in this context, since Passarino and Veltman introduced this notation. However, Veltman used a slightly different convention in several places, like in the definition of the 4-momenta. This introduces multiplicative con-

Fig. C.1 Position of the poles appearing in the integrand of Passarino–Veltman functions, and integration contour chosen to perform the Wick rotation



stands in the definition of the Passarino–Veltman functions. There is even a notation change between Refs. [6, 7]. So, the notation actually used by FormCalc is that given by Ref. [8], which refers to [9] for the details of the dimensional regularization.

The basic idea is to substitute the 4-dimensional integration by an integration over $D = 4 - 2\epsilon$ dimensions. The UV divergences will appear as poles on $\epsilon \rightarrow 0$, but we will be able to reabsorb them in the counter-terms. By definition of dimensional regularization [9], integrals that do not depend on any scale will vanish,

$$\int d^D k \cdot (k^2)^\alpha = 0. \quad (\text{C.2})$$

In contrast, this integral does not exist in the Riemann sense, diverging with the volume $\forall D \in \mathbb{Z}$, $\alpha \in \mathbb{R}$. The integrations rely on a so-called *Wick rotation*, which transforms the integral over Minkowski space to another one over Euclidean space. The trick is making an analytical extension to the complex plane of the *temporal component*, $k^0 = ik_E^0$, and maintaining the *spatial components*, $\vec{k} = \vec{k}_E$.

So, we are dealing with a real $D - 1$ dimensional vector \vec{k} in *space coordinates*, and a *complex* 1-dimensional vector k^0 in time. The Minkowski metric works as expected, $k^2 = (k^0)^2 - \|\vec{k}\|^2$, whose equivalent is $k_E^2 = (k_E^0)^2 + \|\vec{k}\|^2$ in Euler space. As shown in Fig. C.1, because of Cauchy's Theorem, the Wick rotation requires that no pole is present inside the integration region shown in Fig. C.1, and that the contribution of the arcs vanishes in the limit $|k^0| \rightarrow \infty$.

Let us first think about the poles. All interactions in EFT are polynomial at tree level, so the poles can only be due to the denominators of propagating particles. If we take the Feynman prescription for these denominators

$$D_n = \left(k + \sum_{i=1}^{n-1} p_i \right)^2 - m_n^2 + i\varepsilon, \quad \varepsilon \rightarrow 0^+ \quad (\text{C.3})$$

with k, p_i being 4-momenta, then,

$$\operatorname{Re} D_n = \left(\operatorname{Re} k^0 + \sum_{i=1}^{n-1} p_i^0 \right)^2 - (\operatorname{Im} k^0)^2 - \left(\vec{k} + \sum_{i=1}^{n-1} \vec{p}_i \right)^2 - m_n^2 \quad (\text{C.4})$$

$$\operatorname{Im} D_n = 2\operatorname{Im} k^0 \left(\operatorname{Re} k^0 + \sum_{i=1}^{n-1} p_i^0 \right) + \varepsilon, \quad \varepsilon \rightarrow 0^+. \quad (\text{C.5})$$

The zero condition for D_n , which will lead to a pole on the Passarino–Veltman integrand coming from $(1/D_n)$, is $\operatorname{Re} D_n = \operatorname{Im} D_n = 0$. Because they correspond to external (physical, not virtual) particles, they must be on the mass shell, $p_i^0 \geq 0 \forall i$, so that $\operatorname{Im} k^0 \cdot \operatorname{Re} k^0 \leq 0$. $\operatorname{Re} D_n = 0$ means that

$$\left(\operatorname{Re} k^0 + \sum_{i=1}^{n-1} p_i^0 \right)^2 = (\operatorname{Im} k^0)^2 + \left(\vec{k} + \sum_{i=1}^{n-1} \vec{p}_i \right)^2 + m_n^2, \quad (\text{C.6})$$

and there will be *two* solutions, one with $\operatorname{Re} k^0 > 0$ and another one with $\operatorname{Re} k^0 < 0$. So, if simultaneously $\operatorname{Im} D_n = 0$, we extract the value of $\operatorname{Im} k^0$ which, as just shown, will have opposite sign to $\operatorname{Re} k^0$, thus recovering a couple of zeroes (poles of the integrand) marked in Fig. C.1. They always appear in pairs, in the second and fourth quadrant.

The second condition is that the contribution of the arcs shown in Fig. C.1 vanishes in the limit $|k^0| \rightarrow \infty$. Because of the fact that we keep the spatial component \vec{k} finite, the divergence would come from the limit

$$\lim_{|k^0| \rightarrow \infty} \int_{\gamma} d k^0 \frac{1}{(k^0)^{2n}}, \quad (\text{C.7})$$

where n is the number of denominators D_n . But this does vanish for $n \geq 1$. Take $z = k^0 e^{i\theta}$, with $\theta \in [0, \pi/2]$,

$$\int_{\gamma} dz \cdot \frac{1}{z^2} = \int_0^{\pi/2} d(k^0 e^{i\theta}) \frac{1}{(k^0 e^{i\theta})^{2n}} = \int_0^{\pi/2} d\theta \frac{ie^{i(1-2n)\theta}}{(k^0)^{2n-1}} \xrightarrow[n \geq 1]{k^0 \rightarrow \infty} 0. \quad (\text{C.8})$$

Thus, we have proven the two conditions which are necessary for the Wick rotation. Namely, absence of pole contributions in the domain through which the axes are rotated, and convergence to zero of the arch integrals. Now, once in Euclidean space, and using the spherical symmetry of the problem, the integration can be decomposed as

$$\int d^D k_E f(\|k_E\|^2) = \int d k_E \cdot k_E^{D-1} \int d \Omega_D f(k_E^2) = \int d \Omega_D \int d(k_E^2) \cdot \frac{1}{2} (k_E^2)^{(D-4)/2} f(k_E^2), \quad (\text{C.9})$$

where we have used the integral over the surface of the full D-dimensional sphere,

$$\int d\Omega_D = \frac{2\pi^{D/2}}{\Gamma(D/2)}, \quad (\text{C.10})$$

whose proof can be found in Appendix D.1. $\Gamma(x)$ is the Euler’s Gamma function, whose properties can be found, for instance, on Ref. [10].

Furthermore, to maintain consistency while changing the dimension of the integral over the 4-momentum, the integral in Eq. C.9 will be multiplied by a constant μ^{4-D} , where μ has dimensions of momentum k . The divergent Passarino–Veltman functions A_0 and B_0 (Eqs. C.1a and C.1b) already include this constant. Anyway, this will lead to the appearance of an energy scale μ on the final result.

Once all the substitutions completed with the help of the efficient symbolic computations software FORM [7], FormCalc express all the matrix elements as function of the *scalar Passarino–Veltman functions* defined in the four Eq. C.1. Note that, although C_0 and D_0 in Eqs. C.1c and C.1d have very tricky analytical expressions, they are finite. So, no regularization is needed for them. Because $A_0^{(1)}(m)$ and $B_0(p, 0, 0)$ functions in Eqs. C.1a and C.1b are the ones appearing in our computations, we will show here how to compute them. Let us start with $A_0^{(1)}(m)$. By definition,

$$A_0^{(1)}(m) = \frac{\mu^{4-D}}{i\pi^2} \int \frac{d^D k}{(2\pi)^{D-4}} \frac{1}{k^2 - m^2 + i\varepsilon}. \quad (\text{C.11})$$

Doing the Wick rotation, we substitute $k^0 \rightarrow ik_E^0$, $\vec{k} \rightarrow \vec{k}_E$. So,

$$k^2 = (k^0)^2 - \|\vec{k}\|^2 = -(k_E^0)^2 - \|\vec{k}_E\|^2 = -k_E^2, \quad (\text{C.12})$$

and

$$d^D k = dk^0 \cdot d^{D-1} \vec{k} = i dk_E^0 \cdot d^{D-1} \vec{k}_E. \quad (\text{C.13})$$

Thus, taking also into account that $\varepsilon \rightarrow 0^+$, Eq. C.11 transforms to

$$A_0^{(1)}(m) = \frac{\mu^{4-D}}{i\pi^2} \int \frac{i d^D k_E}{(2\pi)^{D-4}} \frac{1}{-k_E^2 - m^2} = -\frac{\mu^{4-D}}{(2\pi)^{D-4}\pi^2} \frac{2\pi^{D/2}}{\Gamma(D/2)} \int_0^\infty dk_E \frac{k_E^{D-1}}{k_E^2 + m^2} \quad (\text{C.14})$$

Making the change of variables $k_e = mx$, $dk_e = m dx$,

$$\begin{aligned} A_0^{(1)}(m) &= -\frac{(2\pi\mu)^{4-D}}{\Gamma(D/2)} 2\pi^{(D-4)/2} \frac{m \cdot m^{D-1}}{m^2} \int_0^\infty dx \frac{x^{D-1}}{x^2 + 1} \\ &= -2\pi^{(D-4)/2} m^{D-2} \frac{(2\pi\mu)^{4-D}}{\Gamma(D/2)} \int_0^\infty dx \frac{x^{D-1}}{x^2 + 1} \end{aligned} \quad (\text{C.15})$$

Now, provided that $D \in (0, 2)$,

$$\int_0^\infty dx \frac{x^{D-1}}{x^2 + 1} = \frac{\pi}{2} \csc \frac{D\pi}{2} = \frac{1}{2} \Gamma\left(1 - \frac{D}{2}\right) \Gamma\left(\frac{D}{2}\right), \quad (\text{C.16})$$

thus we find the result

$$A_0^{(1)}(m) = -m^2 \left(\frac{m^2}{4\pi\mu}\right)^{(D-4)/2} \Gamma\left(1 - \frac{D}{2}\right). \quad (\text{C.17})$$

Now, let us substitute $D = 4 - 2\epsilon$. Take into account that the integral is convergent for $D \in (0, 2)$, which means $\epsilon \in (1, 2)$.

$$A_0^{(1)}(m) = -m^2 \left(\frac{4\pi\mu^2}{m^2}\right)^\epsilon \Gamma(\epsilon - 1) \quad (\text{C.18})$$

It can be seen that this is not well defined for $\epsilon < 1$. However, let us see what happens when we force a Laurent expansion near $\epsilon = 0$,

$$\Gamma(\epsilon - 1) = -\frac{1}{\epsilon} - 1 + \gamma + \mathcal{O}(\epsilon) \quad (\text{C.19})$$

$$A^\epsilon = e^{\epsilon \log A} = 1 + \epsilon \log A + \mathcal{O}(\epsilon^2), \quad (\text{C.20})$$

where $1/\epsilon$ stands for the divergent behaviour near $D = 4$ and $\gamma \approx 0.5772\dots$ is the so-called Euler's constant. So,

$$A_0^{(1)}(m) = m^2 \left(\frac{1}{\epsilon} + 1 - \gamma + \log \frac{4\pi\mu^2}{m^2}\right) = m^2 \left(\Delta - \log \frac{m^2}{\mu^2} + 1\right), \quad (\text{C.21})$$

where $\Delta = (1/\epsilon) - \gamma + \log 4\pi$ is the Δ variable used by FormCalc [3].

For the function $B_0(p^2; 0, 0)$, which appears in the NLO computation, we take the definition Eq. C.1b (particularized to $m_1 = m_2 = 0$),

$$B_0(p^2; 0, 0) = \frac{(2\pi\mu)^{4-D}}{i\pi^2} \int \frac{d^D k}{[k^2 + i\epsilon][(k+p)^2 + i\epsilon]}. \quad (\text{C.22})$$

In order to apply Eq. C.9, we need an integrand which only depends on k_E^2 after the Wick rotation. Note that, in the end, the only operation that we have defined over D -dimensional vectors (with D non-integer, $D \in \mathbb{R} \setminus \mathbb{Z}$) is the integration over the surface of the D -dimensional sphere (Appendix D.1). Here, we do not have a definition of D -dimensional vectors which allows us to explicitly sum them. Thus, we cannot sum $k + p$ and integrate over k on $D \in \mathbb{R} \setminus \mathbb{Z}$ dimensions. Even worse, whatever D -dimensional means, p is a 4-dimensional vector whose components are fixed by external kinematics. To deal with this problem let us assume that, although we are not able to explicitly define such an operation as $k + p$, it is well defined and verify the corresponding algebraic properties. We introduce the *Feynman parametrization* [8], which for the product $1/(D_1 D_2)$ is

$$\frac{1}{D_1 D_2} = \int_0^1 \frac{dx}{[(1-x)D_1 + xD_2]^2}. \quad (\text{C.23})$$

Hence, $B_0(p^2; 0, 0)$ defined in Eq. C.22 is turned into

$$\begin{aligned} B_0(p^2; 0, 0) &= \frac{(2\pi\mu)^{4-D}}{i\pi^2} \int_0^1 dx \int \frac{d^D k}{[(1-x)k^2 + (k+p)^2 x + i\varepsilon]^2} = \\ &= \frac{(2\pi\mu)^{4-D}}{i\pi^2} \int_0^1 dx \int \frac{d^D k}{[k^2 + 2x(kp) + x(p)^2 + i\varepsilon]^2} \end{aligned} \quad (\text{C.24})$$

Now, let us perform the change of variables $k \rightarrow k - xp$, so that

$$k^2 + 2x(kp) + x(p)^2 \xrightarrow{k \rightarrow k - xp} (k - xp)^2 + 2xp(k - xp) + p^2 x = k^2 + x(1-x)p^2 \quad (\text{C.25})$$

When substituting in Eq. C.24,

$$B_0(p^2; 0, 0) = \frac{(2\pi\mu)^{4-D}}{i\pi^2} \int_0^1 dx \int \frac{d^D k}{[k^2 + x(1-x)p^2 + i\varepsilon]^2}, \quad (\text{C.26})$$

where linear combinations of D -dimensional vectors (like $k + p$ in Eq. C.22) do not appear. Next, perform the Wick rotation and change to generalized spherical coordinates in D -dimensions,

$$B_0(p^2; 0, 0) = \frac{(2\pi\mu)^{4-D}}{\pi^2} \frac{2\pi^{D/2}}{\Gamma(D/2)} \int_0^1 dx \int \frac{dk_e \cdot k_e^{D-1}}{[-k^2 + x(1-x)p^2 + i\varepsilon]^2}. \quad (\text{C.27})$$

Let us substitute $D = 4 - 2\epsilon$, and note that we are keeping $\epsilon \neq \varepsilon$. Now, provided $0 < D < 4$ and $\varepsilon > 0$ being small enough ($\varepsilon < x(1-x)p^2$),

$$B_0(p^2; 0, 0) = (4\pi\mu^2)^\epsilon \Gamma(\epsilon) \int_0^1 dx [-x(1-x)p^2 - i\varepsilon]^{-\epsilon}, \quad (\text{C.28})$$

where the integrand is extended to the complex plane by

$$[-x(1-x)p^2 - i\varepsilon]^{-\epsilon} = \exp[-\epsilon \log(-x(1-x)p^2 - i\varepsilon)]. \quad (\text{C.29})$$

This is defined because the logarithm is a complex function with a cut on the left axis. For the sake of simplicity, since $0 \leq x(1-x) \leq 1 \forall x \in [0, 1]$, we redefine ε so that

$$-x(1-x)p^2 - i\varepsilon \rightarrow x(1-x)(-p^2 - i\varepsilon) \quad (\text{C.30})$$

without changing the Riemann sheet where $F(x) = x^{-\epsilon} = e^{-\epsilon \log x}$ is evaluated. Thus, Eq. C.28 turns into

$$\begin{aligned}
B_0(p^2; 0, 0) &= (4\pi\mu^2)^\epsilon (-p^2 - i\varepsilon)^{-\epsilon} \Gamma(\epsilon) \int_0^1 dx [x(1-x)]^{-\epsilon} \\
&= \left(\frac{-p^2 - i\varepsilon}{4\pi\mu^2} \right)^{-\epsilon} \frac{\Gamma(\epsilon) \cdot [\Gamma(1-\epsilon)]^2}{\Gamma(2-2\epsilon)} \quad (\text{C.31})
\end{aligned}$$

And carrying out a power expansion around $\epsilon = 0$,

$$B_0(p^2; 0, 0) = \Delta + 2 - \log \frac{-p^2 - i\varepsilon}{\mu^2} + \mathcal{O}(\epsilon), \quad (\text{C.32})$$

with Δ being $(1/\varepsilon) - \gamma + \log 4\pi$, as it was the case of A_0 .

References

- 1 A. Alloul, N.D. Christensen, C. Degrande, C. Duhr, B. Fuks, FeynRules 2.0 - A complete toolbox for tree-level phenomenology. *Comput. Phys. Commun.* **185**, 2250–2300 (2014)
- 2 T. Hahn, Generating Feynman diagrams and amplitudes with FeynArts 3. *Comput. Phys. Commun.* **140**, 418–431 (2001)
- 3 T. Hahn, M. Perez-Victoria, Automatized one loop calculations in four-dimensions and D-dimensions. *Comput. Phys. Commun.* **118**, 153–165 (1999)
- 4 J.A.M. Vermaseren, New features of FORM. (2000), arXiv:<http://arxiv.org/pdf/math-ph/0010025.pdf> [math-ph]
- 5 C. Degrande, C. Duhr, B. Fuks, D. Grellscheid, O. Mattelaer, T. Reiter, UFO - The universal FeynRules output. *Comput. Phys. Commun.* **183**, 1201–1214 (2012)
- 6 G. Passarino, M. J. G. Veltman, One loop corrections for e^+e^- annihilation into $\mu^+\mu^-$ in the Weinberg model. *Nucl. Phys.* **B160**, 151 (1979)
- 7 G. 't Hooft, M. J. G. Veltman, Scalar one loop integrals. *Nucl. Phys.* **B153**(157), 365–401 (1979)
- 8 M. Böhm, A. Denner, H. Joos, Gauge theories of strong and electroweak interactions; 3rd ed. Trans. of 3rd ed.: *Eichtheorien der starken und elektroschwachen Wechselwirkung*. Stuttgart, Teubner, 2001 (B.G. Teubner, Stuttgart, 2001)
- 9 J.C. Collins, Renormalization: an introduction to renormalization, the renormalization group, and the operator-product expansion, Cambridge monographs on mathematical physics (Cambridge University Press, Cambridge, 1984)
- 10 G.B. Arfken, H.J. Weber, *Mathematical Methods for Physicists*, 6th edn., (Academic Press, New York, NY, 2005)

Appendix D

Several Proofs and Explanations

D.1 Integral over the Surface of a D-Dimensional Sphere

The integral over the surface of the D-dimensional sphere is

$$\int d\Omega_D = \frac{2\pi^{D/2}}{\Gamma(D/2)}, \quad (\text{D.1})$$

where $\Gamma(x)$ is the Euler Gamma function, whose properties can be found in Ref. [1]. Eq. D.1 can be extended to D to the real (and positive) axis, $D \in \mathbb{R}^+$. Let us prove this. Using the identity

$$\int_{-\infty}^{\infty} dx e^{-x^2} = \sqrt{\pi}, \quad (\text{D.2})$$

following Ref. [2], and provided that $D \in \mathbb{N}$ ($D \geq 1$),

$$\begin{aligned} \pi^{D/2} &= \left[\int_{-\infty}^{\infty} dx e^{-x^2} \right]^D = \int d^D \vec{x} \cdot e^{-\|\vec{x}\|^2} = \int d\Omega_D \int_0^{\infty} dx x^{D-1} e^{-x^2} \\ &= \left(\int d\Omega_D \right) \cdot \frac{\Gamma(D/2)}{2}, \end{aligned} \quad (\text{D.3})$$

thus recovering Eq. D.1 only for natural values of D . However, the function $2\pi^{D/2}/\Gamma(D/2)$ is defined also in $D \notin \mathbb{N}$, because it is a composition of analytic functions in the complex plane.⁵ Thus, the analytic extension of Eq. D.1 to the complex plane is trivial.

⁵See Ref. [1] for more details. Special care should be taken for $n = 0, -1, -2, \dots$ ($D = 0, -1/2, -1/3, \dots$), where $\Gamma(n)$ has single poles. However, this does not affect our computations, since we always have real and positive values of D .

D.2 Integration of Legendre Polynomials

Equation 4.29,

$$\begin{aligned} \int_0^{2\pi} d\tilde{\varphi} \int_0^\pi d\tilde{\theta} \cdot \sin \tilde{\theta} \cdot P_J[\cos \tilde{\theta}] \cdot P_{J'}[\cos \theta \cos \tilde{\theta} + (-1)^n \sin \theta \sin \tilde{\theta} \cos \tilde{\varphi}] = \\ = \frac{4\pi}{2J+1} \delta_{J,J'} P_J[\cos \theta], \end{aligned} \quad (\text{D.4})$$

can be easily proven taking into account the *Addition Theorem for Spherical Harmonics*,⁶

$$\cos \gamma \equiv \cos \theta_1 \cos \theta_2 + \sin \theta_1 \sin \theta_2 \cos(\varphi_1 - \varphi_2) \quad (\text{D.5})$$

$$P_J(\cos \gamma) = \frac{4\pi}{2J+1} \sum_{m=-J}^J (-1)^m Y_J^m(\theta_1, \varphi_1) Y_J^{-m}(\theta_2, \varphi_2) \quad (\text{D.6})$$

$$\begin{aligned} &= P_J(\cos \theta_1) P_J(\cos \theta_2) \\ &+ 2 \sum_{m=1}^J \frac{(J-m)!}{(J+m)!} P_J^m(\cos \theta_1) P_J^m(\cos \theta_2) \cos[m(\varphi_1 - \varphi_2)] \end{aligned} \quad (\text{D.7})$$

Just take $\theta_1 \rightarrow \tilde{\theta}$, $\theta_2 \rightarrow \theta$, $\varphi_1 \rightarrow \tilde{\varphi}$, $\varphi_2 \rightarrow n\pi$, considering that $\cos(\tilde{\varphi} - n\pi) = (-1)^n \cos \tilde{\varphi} \forall n \in \mathbb{Z}$. Now,

$$\int_0^{2\pi} d\tilde{\varphi} \cos[m(\tilde{\varphi} - n\pi)] = \frac{1}{m} \sin[m(\tilde{\varphi} - n\pi)] \Big|_{\tilde{\varphi}=0}^{2\pi} = 0 \forall m \in \mathbb{Z}, \quad (\text{D.8})$$

so that the integration of Eq. 4.29 reduces to

$$2\pi \int_0^\pi d\tilde{\theta} \cdot \tilde{\theta} \cdot P_J[\cos \tilde{\theta}] P_{J'}(\cos \tilde{\theta}) P_J(\cos \theta) \quad (\text{D.9})$$

And now, because of the orthonormality of Legendre polynomials [1],

$$\int_{-1}^1 dx \cdot P_J(x) P_{J'}(x) = \frac{2}{2J+1} \delta_{J,J'}, \quad (\text{D.10})$$

we recover trivially Eq. 4.29 when integrating over $\tilde{\theta}$.

⁶For a proof of this theorem refer, for example, to [1].

D.3 Integrals for the N/D Method

In order to compute the integrals of Eq. 4.129, let us first consider the following ones,

$$I_1(y, y_1, y_2) = \int_{y_1}^{y_2} \frac{dx}{x(x-y)} = \int_{y_1}^{y_2} dx \frac{1}{y} \left[\frac{1}{x-y} - \frac{1}{x} \right] = \frac{1}{y} \log \left(1 - \frac{y}{x} \right) \Big|_{x=y_1}^{y_2} \quad (\text{D.11a})$$

$$I_2(y, y_1, y_2) = \int_{y_1}^{y_2} \frac{dx}{x^2(x-y)} = \frac{1}{y^2} \left[\log \left(1 - \frac{y}{x} \right) + \frac{y}{x} \right] \Big|_{x=y_1}^{y_2} \quad (\text{D.11b})$$

$$\tilde{I}'_1(y, y_1, y_2) = \int_{y_1}^{y_2} \frac{dx \log x}{x(x-y)} = 2 \log x \log \left(1 - \frac{x}{y} \right) + \log^2 x + 2\text{Li}_2 \left(\frac{x}{y} \right) \Big|_{x=y_1}^{y_2}, \quad (\text{D.11c})$$

where $\text{Li}_2(\eta)$ is the dilogarithm function,⁷ defined as

$$\text{Li}_2(x) \equiv \sum_{n=1}^{\infty} \frac{x^n}{n^2}, \quad |x| \leq 1. \quad (\text{D.12})$$

For $|x| > 1$, the dilogarithm is defined by an analytic continuation. Anyway, according to Refs. [3, 4], this analytic continuation can be embodied in an integrate form

$$\text{Li}_2(x) = - \int_0^x \frac{\log(1-t)}{t} dt, \quad (\text{D.13})$$

and its asymptotic form for large values of x , necessary in order to compute the limit $\Lambda \rightarrow \infty$ in Eq. D.11c,

$$\text{Li}_2(z) \xrightarrow[\text{Im } z \rightarrow 0^+]{z \rightarrow \infty} \frac{\pi^2}{3} - \frac{1}{2} \log^2 z + i\pi \log z, \quad (\text{D.14})$$

provided that $z = \text{Re}(z) + i\epsilon$, where $\epsilon \rightarrow 0^+$. If, on the other had, we had $z = \text{Re}(z) - i\epsilon$ ($\epsilon \rightarrow 0^+$), then the correct asymptotic form would be

$$\text{Li}_2(z) \xrightarrow[\text{Im } z \rightarrow 0^-]{z \rightarrow \infty} \frac{\pi^2}{3} - \frac{1}{2} \log^2 z - i\pi \log z. \quad (\text{D.15})$$

Note that this last case ($z = \text{Re}(z) - i\epsilon$, $\epsilon \rightarrow 0^+$) is the one which, indeed, appears in Eq. D.11c. Take into account that $y_2 \rightarrow \infty$, and $y \equiv (s + i\epsilon)/\mu^2$ (with $\text{Im } y \rightarrow 0^+$) appears on the denominator, so that $\text{Im}(y_2/y) \rightarrow 0^-$.

⁷See, for example, Refs. [3, 4].

If the limits $y_2 \rightarrow \infty$ are computed in Eq. D.11, then those expressions turn into

$$I_1(y, y_1, \infty) = -\frac{1}{y} \log \left(1 - \frac{y}{y_1} \right) \quad (\text{D.16a})$$

$$I_2(y, y_1, \infty) = -\frac{1}{y^2} \left[\frac{y}{y_1} + \log \left(1 - \frac{y}{y_1} \right) \right] \quad (\text{D.16b})$$

$$I'_1(y, y_1, \infty) = -\frac{1}{y} \left[\frac{1}{2} \log^2(-y) + \text{Li}_2 \frac{y_1}{y} - \frac{1}{2} \log^2(y_1) + \log y_1 \log \left(1 - \frac{y_1}{y} \right) + \frac{\pi^2}{6} \right], \quad (\text{D.16c})$$

Now, let us effect the change of variables $y = (s + i\epsilon)/\mu^2$, $x = s'/\mu^2$, $y_1 = m^2/\mu^2$, $y_2 = \Lambda^2/\mu^2$. The integrals of Eq. D.11 and their solutions when $\Lambda^2 \rightarrow \infty$ and $\epsilon \rightarrow 0^+$ (Eq. D.16) turn into

$$\begin{aligned} \frac{1}{\mu^2} I_1(y, y_1, y_2) &= \frac{1}{\mu^2} \int_{y_1}^{y_2} \frac{dx}{x(x-y)} = \int_{m^2}^{\Lambda^2} \frac{ds'}{s'(s' - s - i\epsilon)} \quad \xrightarrow[y_2 \rightarrow \infty]{\Lambda^2 \rightarrow \infty} -\frac{1}{s} \log \left(1 - \frac{s}{m^2} \right) \\ \frac{1}{\mu^4} I_2(y, y_1, y_2) &= \frac{1}{\mu^2} \int_{y_1}^{y_2} \frac{dx}{x^2(x-y)} = \frac{1}{\mu^4} \int_{\mu^2}^{\Lambda^2} \frac{ds'}{(s')^2(s' - s - i\epsilon)} \\ &\quad \xrightarrow[y_2 \rightarrow \infty]{\Lambda^2 \rightarrow \infty} -\frac{1}{s^2} \left[\frac{s}{m^2} + \log \left(1 - \frac{s}{m^2} \right) \right] \end{aligned} \quad (\text{D.17a})$$

$$\begin{aligned} \frac{1}{\mu^2} I'_1(y, y_1, y_2) &= \frac{1}{\mu^2} \int_{y_1}^{y_2} \frac{dx \log x}{x(x-y)} = \int_{m^2}^{\Lambda^2} \frac{ds' \log \frac{s'}{\mu^2}}{s'(s' - s - i\epsilon)} \quad (\text{D.17b}) \\ &\quad \xrightarrow[y_2 \rightarrow \infty]{\Lambda^2 \rightarrow \infty} -\frac{1}{s} \left[\frac{1}{2} \log^2 \left(\frac{-s}{\mu^2} \right) + \text{Li}_2 \frac{m^2}{s} - \frac{1}{2} \log^2 \left(\frac{m^2}{\mu^2} \right) + \log \frac{m^2}{\mu^2} \log \left(1 - \frac{m^2}{s} \right) + \frac{\pi^2}{6} \right]. \end{aligned} \quad (\text{D.17c})$$

These expressions allow us to recover Eq. 4.129, as expected.

D.4 Comparison of Our Elastic $\omega\omega$ Partial Waves with a Higgsless ECL Model

Before the discovery of the Higgs boson at the LHC, several authors ([5-7]) motivated a strongly interacting regime for the dynamics of the EWSBS to solve some of the problems for which the Higgs boson was postulated. In particular, we will quote Ref. [8] since, although they worked in the Higgsless ECL model, they have computed the real part of the NLO partial waves (including the tensor-isotensor channel $IJ = 22$), and their results can be used to check our elastic WBGBs partial waves of Eqs. 3.136–3.140, taking $a = b = 0$ in our expressions.

Furthermore, Ref. [8] (and its extension [9]) are particularly encouraging since they are interested in the implementation of strongly interacting theories into their own MonteCarlo program, WHIZARD [10, 11].

However, while we take the non-linear electroweak chiral Lagrangian with an arbitrary function for the couplings of the Higgs-like particle with the EWSBS,⁸

$$\mathcal{L}_2 = \frac{v^2}{4} \left(1 + 2a \frac{h}{v} + b \left(\frac{h}{v} \right)^2 + \dots \right) \text{Tr}[(D_\mu U)^\dagger D^\mu U] + \dots, \quad (\text{D.18})$$

Ref. [8] takes the Higgsless regime $a = b = 0$,

$$\mathcal{L}_2 = \frac{v^2}{4} \text{Tr}[(D_\mu U)^\dagger D^\mu U]. \quad (\text{D.19})$$

Note that the work of Ref. [8] has been extended (see Ref. [9] for example), but apparently a non-linear chiral Lagrangian of the form of Eq. 2.31, has not been considered. In particular, Ref. [8] introduces the Higgs-like particle through their Eq. 1,

$$\mathbf{H} \rightarrow \frac{1}{2}(v + h)\Sigma \quad (\text{D.20})$$

where Σ is the non-linear Goldstone-boson representation. Apparently, they are not considering a more general coupling with the Higgs-like boson, with a factor like (a, b) (see this work, Eq. 2.6; and some other works like Ref. [12]), the c_W (see Ref. [13]), the $F_U(h)$ (see Ref. [14] and their Eq. 5),...

Anyway, we are interested in Eqs. 4.13 and 4.14 from Ref. [8]. They should be compatible with the real part of our $\omega\omega \rightarrow \omega\omega$ partial waves (Eqs. 3.136–3.140, see also the definition of Eq. 3.132). Provided that we define $a = b = 0$, in our equations, and consider that the definition of partial wave of Ref. [8] (see their Eqs. 4.11 and 4.12) should be multiplied by $1/(32\pi)$ to match the definition of partial wave which we use ($K = 2$ in Eqs. 3.123 and 3.124). This is an independent check of our NLO and partial waves computation.

Note that, when the real part of our amplitudes is taken, because we are working over the RC (physical zone, $s' = s + i\epsilon$, $s > 0$, $\epsilon \rightarrow 0^+$), we have $\text{Re} \log(s/\mu^2) = \log(s/\mu^2)$, $\text{Re} \log(-s/\mu^2) = \log(s/\mu^2)$. Thus, once we define $a = b = 0$, in our equations (Eqs. 3.136–3.140), and we multiply them by 32π , we find that

⁸See our Eq. 2.4 and the phenomenological Lagrangian of Eq. 2.31.

$$A_{00}^{(0)} = 32\pi K_{00}s \Big|_{a=b=0} = \frac{3s}{v^2} \quad (\text{D.21a})$$

$$A_{11}^{(0)} = \frac{s}{3v^2} \quad (\text{D.21b})$$

$$A_{20}^{(0)} = -\frac{s}{v^2} \quad (\text{D.21c})$$

$$A_{02}^{(0)} = A_{22}^{(0)} = 0, \quad (\text{D.21d})$$

thus being compatible with Eq. 4.13 from Ref. [8]. Now, let us compute the real part of our NLO results, (with $a = b = 0$, $a_4 = \alpha_4$, $a_5 = \alpha_5$)

$$\text{Re } A_{00}^{(1)} = \left[\frac{8}{3}(7a_4(\mu) + 11a_5(\mu)) - \frac{25}{144\pi^2} \log \frac{s}{\mu^2} + \frac{101}{288\pi^2} \right] \frac{s^2}{v^4} \quad (\text{D.22a})$$

$$\text{Re } A_{11}^{(1)} = \left[\frac{4}{3}(a_4(\mu) - 2a_5(\mu)) + \frac{1}{432\pi^2} \right] \frac{s^2}{v^4} \quad (\text{D.22b})$$

$$\text{Re } A_{20}^{(1)} = \left[\frac{16}{3}(2a_4(\mu) + a_5(\mu)) - \frac{5}{72\pi^2} \log \frac{s}{\mu^2} + \frac{91}{576\pi^2} \right] \frac{s^2}{v^4} \quad (\text{D.22c})$$

$$\text{Re } A_{02}^{(1)} = \left[\frac{8}{15}(2a_4(\mu) + a_5(\mu)) - \frac{1}{144\pi^2} \log \frac{s}{\mu^2} + \frac{1}{90\pi^2} \right] \frac{s^2}{v^4} \quad (\text{D.22d})$$

$$\text{Re } A_{22}^{(1)} = \left[\frac{4}{15}(a_4(\mu) + 2a_5(\mu)) - \frac{1}{360\pi^2} \log \frac{s}{\mu^2} + \frac{71}{28800\pi^2} \right] \frac{s^2}{v^4}. \quad (\text{D.22e})$$

Our computations (Eq. D.22) coincide with Ref. [8]. The LO, NLO logarithm terms and the coefficients of the NLO parameters $\alpha_4(\mu)$ and $\alpha_5(\mu)$ (our a_4 and a_5) are the same. The non-logarithm term which is $\propto s^2/v^4$ appears to be incompatible, but note that this is due to a different renormalization of the $\alpha_4(\mu)$ and $\alpha_5(\mu)$ parameters. Our running equations for $a_4^r(\mu)$ and $a_5^r(\mu)$ (Eqs. 3.42a and 3.42b), taking $a = b = 0$, are compatible with those for $\alpha_4(\mu)$ and $\alpha_5(\mu)$ (Eq. 4.6 from Ref. [8]). But we have taken different values for $a_4(\mu_0)$ and $a_5(\mu_0)$. Thus, in order to have full agreement, it is necessary to introduce

$$a_4(\mu) - \alpha_4(\mu) = a_4(\mu_0) - \alpha_4(\mu_0) = \frac{13}{1152\pi^2} \quad (\text{D.23a})$$

$$a_5(\mu) - \alpha_5(\mu) = a_5(\mu_0) - \alpha_5(\mu_0) = \frac{5}{1152\pi^2}. \quad (\text{D.23b})$$

This is an additional check to our expressions (Eq. D.22). Note that, when comparing with the results from other works, it is necessary to take into account possible differences in the definition of $a_4(\mu_0)$ and $a_5(\mu_0)$, as in Eq. D.23.

D.5 Concerns About the Applicability Conditions of the ET

Many references from the 90's studied the limits of applicability of the equivalence theorem [15–22], arriving to the conclusion that it is valid also for the particular case of the chiral Lagrangian. This allows us to use the ET in this dissertation.

As an instance of a suggested counterexample of the ET, Ref. [23] claimed that, for certain kind of technicolor models, the ET would be violated. Such a violation would come from a *global anomaly* through the triangle fermion loop. That is, from the vertex $Z_L^0 - \gamma - \gamma^*$, γ^* being a virtual photon. As clarified in Ref. [24], the key point is that the $\pi^0 \rightarrow \gamma\gamma$ amplitude violates the ET only in the zero momentum limit due to its low energy nature, but not in the high energy limit case ($E \gg M_W$). This is a very important concern, since any computation of low-energy events like the decay of a SM-like Higgs boson cannot be computed with techniques that involve the usage of the ET. Only hard scattering events, like scattering of gauge bosons can. Hence, Ref. [24] restated the validity of the ET for the particular case of chiral Lagrangians at sufficient energy.

References

- 1 G.B. Arfken, H.J. Weber, *Mathematical Methods for Physicists*, 6th edn. (Academic Press, New York, NY, 2005)
- 2 M.E. Peskin, D.V. Schroeder, *An Introduction to Quantum Field Theory; 1995 ed* (Westview, Boulder, CO, 1995)
- 3 G.E. Andrews, R.A. Askey, R. Roy, *Special Functions*, 2nd edn., Encyclopaedia of Mathematics and its Applications (Cambridge University Press, Cambridge, 2001)
- 4 L. Lewin, Polylogarithms and associated functions (North-Holland, New York, NY, 1981)
- 5 T. Appelquist, C.W. Bernard, Strongly interacting Higgs Bosons. Phys. Rev. **D22**, 200 (1980)
- 6 A.C. Longhitano, Heavy Higgs Bosons in the Weinberg-Salam model. Phys. Rev. **D22**, 1166 (1980)
- 7 A.C. Longhitano, Low-energy impact of a heavy Higgs Boson sector. Nucl. Phys. **B188**, 118 (1981)
- 8 A. Alboteanu, W. Kilian, J. Reuter, Resonances and unitarity in Weak Boson scattering at the LHC. JHEP **11**, 010 (2008)
- 9 W. Kilian, T. Ohl, J. Reuter, M. Sekulla, High-energy vector Boson scattering after the Higgs discovery. Phys. Rev. **D91**, 096007 (2015)
- 10 W. Kilian, T. Ohl, J. Reuter, WHIZARD: simulating multi-particle processes at LHC and ILC. Eur. Phys. J. **C71**, 1742 (2011)
- 11 M. Moretti, T. Ohl, J. Reuter, O'Mega: an optimizing matrix element generator. 1981–2009 (2001), arXiv:<http://arxiv.org/abs/hep-ph/0102195> [hep-ph]
- 12 D. Espriu, F. Mescia, Unitarity and causality constraints in composite Higgs models. Phys. Rev. **D90**, 015035 (2014)
- 13 R. Contino, M. Ghezzi, C. Grojean, M. Muhlleitner, M. Spira, Effective Lagrangian for a light Higgs-like scalar. JHEP **07**, 035 (2013)
- 14 G. Buchalla, O. Catà, C. Krause, Complete Electroweak Chiral Lagrangian with a Light Higgs at NLO. Nucl. Phys. **B880**, 552–573 (2014)
- 15 W.B. Kilgore, Anomalous condensates and the equivalence theorem. Phys. Lett. **B323**, 161–168 (1994)

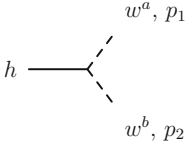
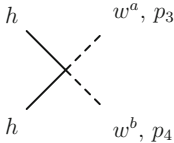
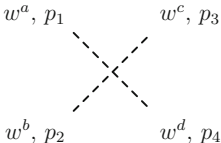
- 16 P.B. Pal, Equivalence theorem and dynamical symmetry breaking. Phys. Lett. **B321**, 229–233 (1994)
- 17 P.B. Pal, What is the equivalence theorem really? (1994), arXiv:<http://arxiv.org/abs/hep-ph/9405362> [hep-ph]
- 18 X. Zhang, A Remark on the Yukawa sector of the standard model. Phys. Rev. **D43**, 3768–3770 (1991)
- 19 A. Dobado, J.R. Pelaez, M.T. Urdiales, Applicability constraints of the equivalence theorem. Phys. Rev. **D56**, 7133–7142 (1997)
- 20 A. Dobado, J.R. Pelaez, M.T. Urdiales, The Applicability of the equivalence theorem in χ (PT), in 27th International Conference on High-energy Physics (ICHEP 94) Glasgow, Scotland, July 20–27, 1994 (1994), arXiv:<http://arxiv.org/abs/hep-ph/9407384> [hep-ph]
- 21 A. Dobado, J.R. Pelaez, On The Equivalence theorem in the chiral perturbation theory description of the symmetry breaking sector of the standard model. Nucl. Phys. **B425**, [Erratum: Nucl. Phys. **B434**, 475 (1995)], 110–136 (1994)
- 22 A. Dobado, J.R. Pelaez, The Equivalence theorem for chiral lagrangians. Phys. Lett. **B329**, [Addendum: Phys. Lett. **B335**, 554 (1994)], 469–478 (1994)
- 23 J.F. Donoghue, J. Tandean, The Equivalence theorem and global anomalies. Phys. Lett. **B301**, 372–375 (1993)
- 24 H.-J. He, Y.-P. Kuang, X.-y. Li, Proof of the equivalence theorem in the chiral Lagrangian formalism. Phys. Lett. **B329**, 278–284 (1994)

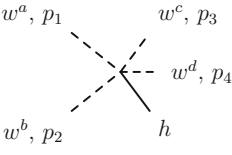
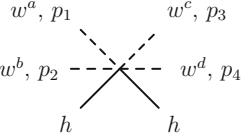
Appendix E

Feynman Diagrams for the Effective Lagrangian

All the necessary vertices have been computed both by hand and by using the program FeynRules [1], as explained in p. 41. The FeynRules convention is followed, thus our vertices correspond to $i\mathcal{M}$, where \mathcal{M} is the scattering amplitude.

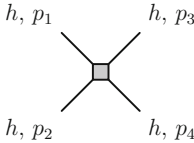
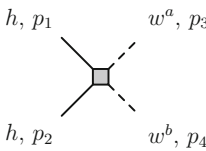
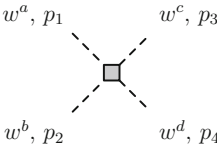
E.1 $\omega\omega$ Scattering, Isospin Basis, LO Coefficients

Vertex	Feynman diagram
	$-\frac{2ia}{v}(p_1p_2)\delta_{a,b}$
	$-\frac{2ib}{v^2}(p_3p_4)\delta_{a,b}$
	$-\frac{i}{v^2}\{[p_1p_3 + p_1p_4 + p_2p_3 + p_2p_4]\delta_{a,b}\delta_{c,d} \\ + [p_1p_2 + p_1p_4 + p_3p_2 + p_3p_4]\delta_{a,c}\delta_{b,d} \\ + [p_1p_2 + p_1p_3 + p_4p_2 + p_4p_3]\delta_{a,d}\delta_{b,c}\}$

Vertex	Feynman diagram
	$-\frac{2ia}{v^3} \{ [p_1 p_3 + p_1 p_4 + p_2 p_3 + p_2 p_4] \delta_{a,b} \delta_{c,d} \\ + [p_1 p_2 + p_1 p_4 + p_3 p_2 + p_3 p_4] \delta_{a,c} \delta_{b,d} \\ + [p_1 p_2 + p_1 p_3 + p_4 p_2 + p_4 p_3] \delta_{a,d} \delta_{b,c} \}$
	$-\frac{2ib}{v^4} [(p_1 p_3 + p_1 p_4 + p_2 p_3 + p_2 p_4) \delta_{a,b} \delta_{c,d} \\ + (p_1 p_2 + p_1 p_4 + p_3 p_2 + p_3 p_4) \delta_{a,c} \delta_{b,d} \\ + (p_1 p_2 + p_1 p_3 + p_4 p_2 + p_4 p_3) \delta_{a,d} \delta_{b,c}]$

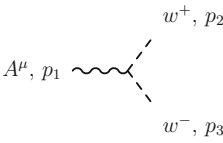
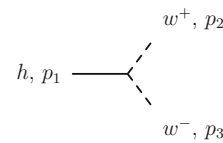
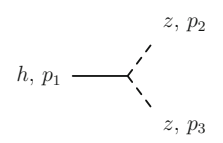
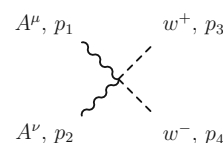
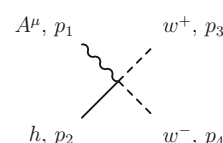
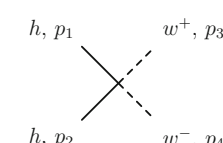
These vertices correspond to the effective Lagrangian of Eq. 2.31. The vertices where the NLO counterterms a_4 , a_5 , d , e and g appear will be given in the next subsection.

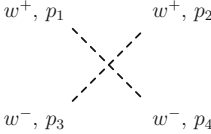
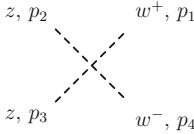
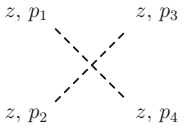
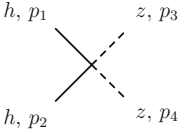
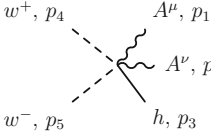
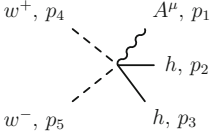
E.2 $\omega\omega$ Scattering, Isospin Basis, NLO Coefficients

Vertex	Feynman diagram
	$\frac{8ig}{v^4} [(p_1 p_2)(p_3 p_4) + (p_1 p_3)(p_2 p_4) + (p_1 p_4)(p_2 p_3)]$
	$\frac{4ie}{v^4} [(p_1 p_4)(p_2 p_3) + (p_1 p_3)(p_2 p_4)] \delta_{a,b} \\ + \frac{8id}{v^4} [(p_1 p_2)(p_3 p_4)] \delta_{a,b}$
	$\frac{16ia_4}{v^4} \{ [(p_1 p_3)(p_2 p_4) + (p_1 p_4)(p_2 p_3)] \delta_{a,b} \delta_{c,d} \\ + [(p_1 p_2)(p_3 p_4) + (p_1 p_4)(p_2 p_3)] \delta_{a,c} \delta_{b,d} \\ + [(p_1 p_2)(p_3 p_4) + (p_1 p_3)(p_2 p_4)] \delta_{a,d} \delta_{b,c} \} \\ + \frac{32ia_5}{v^4} \{ [(p_1 p_2)(p_3 p_4)] \delta_{a,b} \delta_{c,d} \\ + [(p_1 p_3)(p_2 p_4)] \delta_{a,c} \delta_{b,d} + [(p_1 p_4)(p_2 p_3)] \delta_{a,d} \delta_{b,c} \}$

The shown vertices correspond to the effective Lagrangian of Eq. 2.31. We include only the vertices where the NLO counterterms a_4 , a_5 , d , e and g appear.

E.3 $\gamma\gamma$ Scattering, Charge Basis, LO

Vertex	Exponential	Spherical
	$ie(p_{2\mu} - p_{3\mu})$	$ie(p_{2\mu} - p_{3\mu})$
	$-\frac{2ia}{v}(p_2 p_3)$	$-\frac{2ia}{v}(p_2 p_3)$
	$-\frac{2ia}{v}p_2 p_3$	$-\frac{2ia}{v}p_2 p_3$
	$2ie^2 g_{\mu\nu}$	$2ie^2 g_{\mu\nu}$
	$\frac{2iae}{v}(p_{3\mu} - p_{4\mu})$	$\frac{2iae}{v}(p_{3\mu} - p_{4\mu})$
	$-\frac{2ib}{v^2}p_3 p_4$	$-\frac{2ib}{v^2}p_3 p_4$

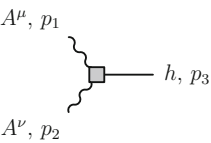
Vertex	Exponential	Spherical
	$-\frac{i}{3v^2}[2(p_1p_2 + p_3p_4) + (p_1 + p_2)^2]$	$-\frac{i}{v^2}[2(p_1p_2 + p_3p_4) - (p_1 + p_2)^2]$
	$\frac{i}{3v^2}[2(p_1p_4 + p_2p_3) + (p_1 + p_4)^2]$	$\frac{i}{v^2}(p_1 + p_4)^2$
	0	$-\frac{2i}{v^2}[p_1p_4 + p_2p_3 - (p_1 + p_4)^2]$
	$-\frac{2ib}{v^2}p_3p_4$	$-\frac{2ib}{v^2}p_3p_4$
	$\frac{4iae^2}{v}g_{\mu\nu}$	$\frac{4iae^2}{v}g_{\mu\nu}$
	$\frac{2ibc}{v^2}(p_{4\mu} - p_{5\mu})$	$\frac{2ibc}{v^2}(p_{4\mu} - p_{5\mu})$

Vertex	Exponential	Spherical
	$\frac{2ie}{3v^2}(p_{5\mu} - p_{2\mu})$	0
	$\frac{4ie}{3v^2}(p_{5\mu} + p_{4\mu} - p_{3\mu} - p_{2\mu})$	0
	$\frac{4ibc^2}{v^2}g_{\mu\nu}$	$\frac{4ibc^2}{v^2}g_{\mu\nu}$

These vertices correspond to the effective Lagrangian of Eq. 2.33 (for the exponential parametrization) and Eq. 2.34 (for the spherical parametrization). The vertices where the NLO counterterms a_1 , a_2 , a_3 and c_γ appear will be given in the next subsection. Note that, on the contrary, the NLO counterterms which do not contain any photons (d , e and g) do appear in this table. Some diagrams are very similar to those listed on Appendix E.1, but note the change of basis (from isospin to charge one). We also omit the diagrams which are not necessary for $\gamma\gamma$ scattering.

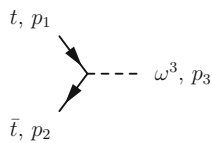
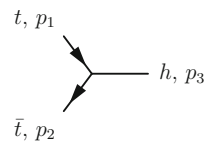
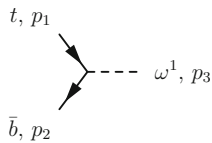
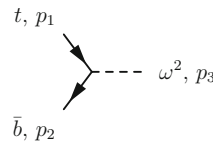
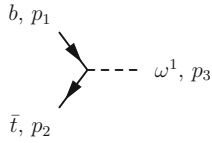
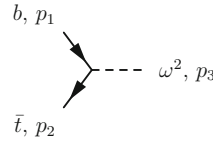
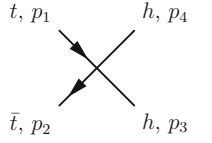
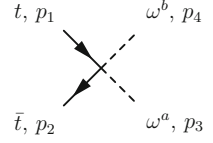
E.4 $\gamma\gamma$ Scattering, Charge Basis, NLO

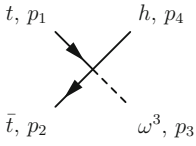
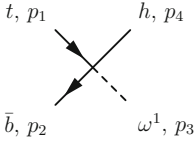
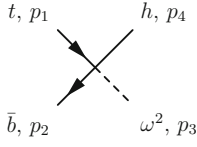
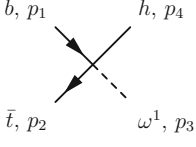
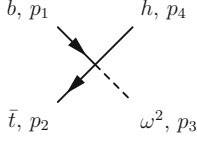
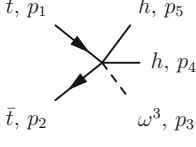
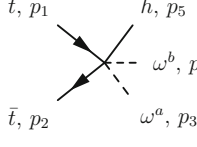
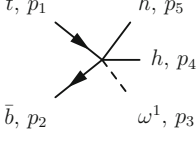
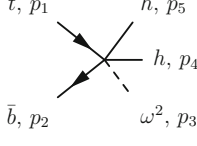
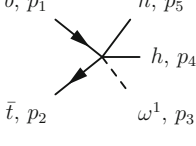
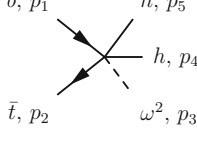
Vertex	Exponential	Spherical
	$-\frac{4ie(a_3-a_2)}{v^2}[(p_1p_3)p_{2\mu} - (p_1p_2)p_{3\mu}]$	Same than Expon.
	$\begin{aligned} &\frac{8ie^2a_1}{v^2}[(p_1p_2)g_{\mu\nu} - p_{2\mu}p_{1\nu}] \\ &+ \frac{4ie^2(a_3-a_2)}{v^2}[(p_1+p_2)^2g_{\mu\nu} \\ &\quad - (p_{1\mu}+p_{2\mu})p_{1\nu} \\ &\quad - p_{2\mu}(p_{1\nu}+p_{2\nu})] \end{aligned}$	Same than Expon.

Vertex	Exponential	Spherical
	$\frac{2ic_\gamma}{v} [(p_1 p_2) g_{\mu\nu} - p_{2\mu} p_{1\nu}]$	Same than Expon.

These vertices correspond to the effective Lagrangian of Eq. 2.33 (for the exponential parametrization) and Eq. 2.34 (for the spherical parametrization). We include only the vertices where the NLO counterterms a_1 , a_2 , a_3 and c_γ appear.

E.5 $t\bar{t}$ in the Final State, Isospin Basis

Vertex	Feynman diagram	Vertex	Feynman diagram
	$\frac{M_t}{v} \gamma^5$		$-i \frac{c_1 M_t}{v}$
	$\frac{M_t}{v} P_R$		$\frac{iM_t}{v} P_R$
	$-\frac{M_t}{v} P_L$		$\frac{iM_t}{v} P_L$
	$-\frac{2iM_t c_2}{v^2}$		$\frac{iM_t}{v^2} \delta_{a,b}$

Vertex	Feynman diagram	Vertex	Feynman diagram
	$\frac{M_t c_1}{v^2} \gamma^5$		
	$\frac{M_t c_1}{v^2} P_R$		$\frac{i M_t c_1}{v^2} P_R$
	$-\frac{M_t c_1}{v^2} P_L$		$\frac{i M_t c_1}{v^2} P_L$
	$\frac{2 M_t c_2}{v^3} \gamma^5$		$\frac{i M_t c_1}{v^3} \delta_{a,b}$
	$\frac{2 M_t c_2}{v^3} P_R$		$\frac{2 i M_t c_2}{v^3} P_R$
	$-\frac{2 M_t c_2}{v^3} P_L$		$\frac{2 i M_t c_2}{v^3} P_L$

Vertex	Feynman diagram	Vertex	Feynman diagram
	$\frac{2iM_t c_2}{v^4} \delta_{a,b}$		

Reference

1 A. Alloul, N.D. Christensen, C. Degrande, C. Duhr, B. Fuks, FeynRules 2.0 - A complete toolbox for tree-level phenomenology. Comput. Phys. Commun. **185**, 2250–2300 (2014)

Appendix F

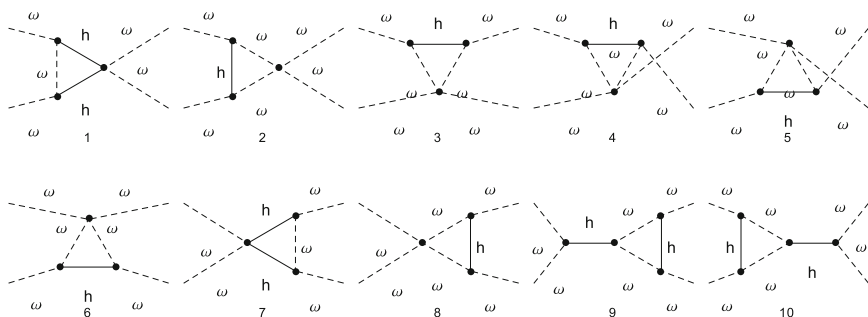
One-Loop Feynman Diagrams

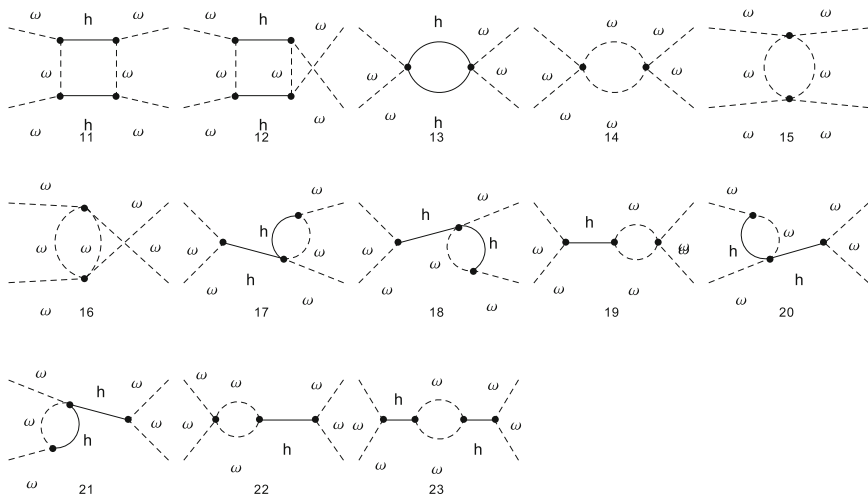
This Appendix contains all the NLO Feynman diagrams which enter in the computations. All the tadpoles have been omitted, since we are neglecting all the masses of particles inside the loops and lacking a scale, they vanish because of Eq. C.2. These diagrams have been drawn with FeynArts [1] and generated with FeynRules [2], FeynArts [1] and FormCalc [3, 4], as explained in p. 41.

F.1 $\omega\omega$

These computations are based on the spherical parameterization and the isospin basis is used. See Eq. 2.31 for the Lagrangian and Appendices E.1 and E.2 for the Feynman rules.

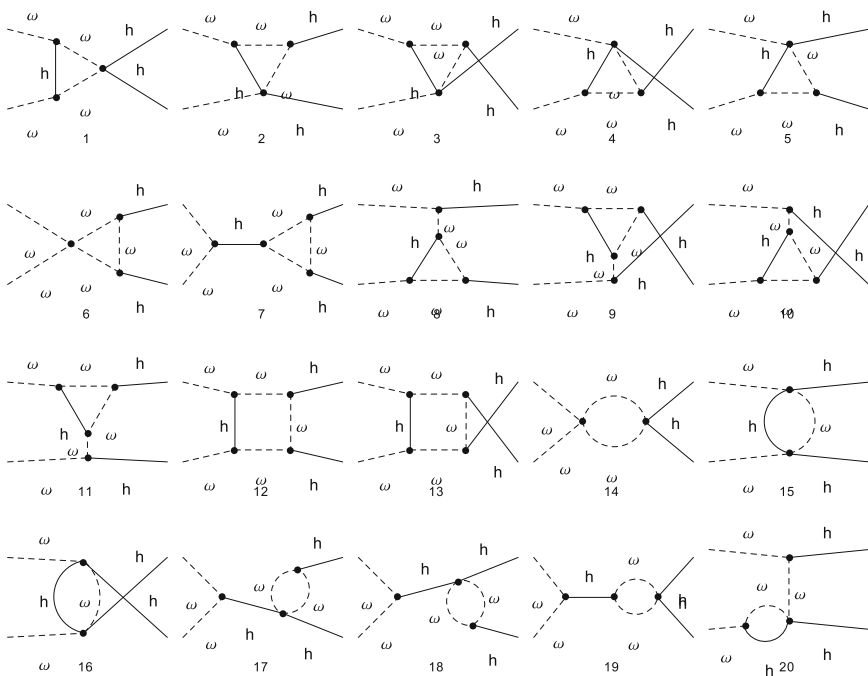
F.1.1 $\omega\omega \rightarrow \omega\omega$

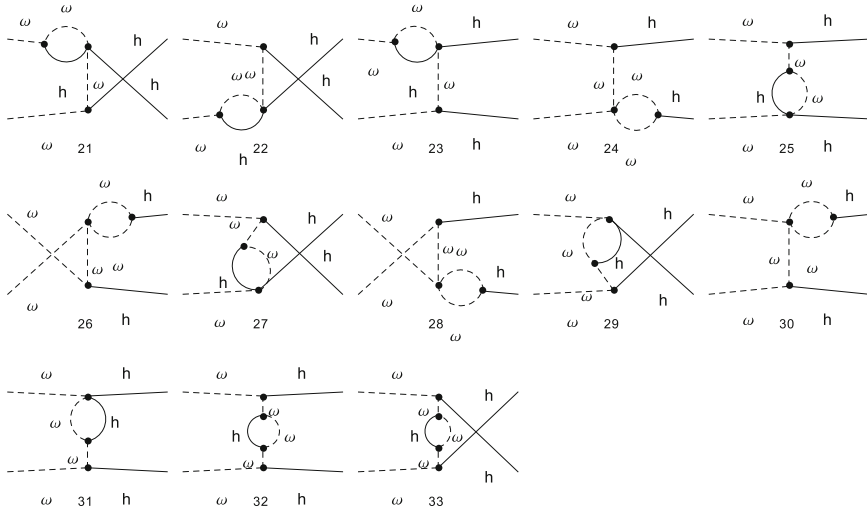




Diagrams used to obtain the amplitude of Eq. 3.32.

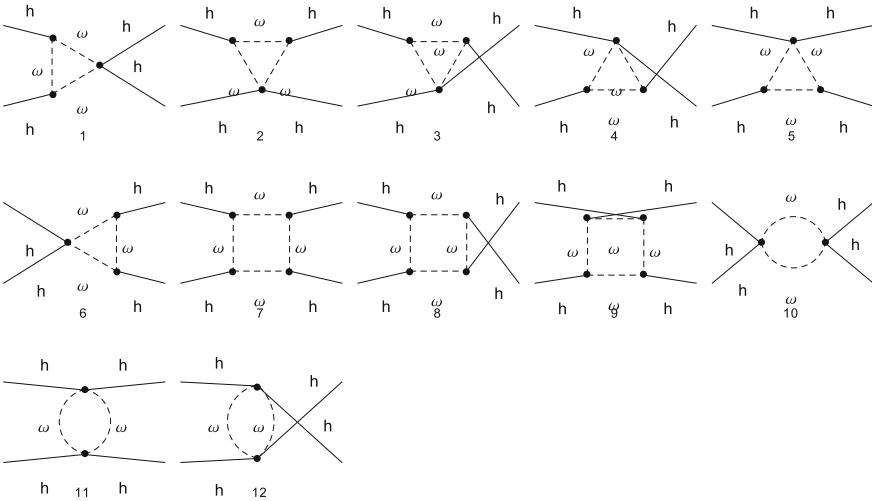
F.1.2 $\omega\omega \rightarrow hh$





Diagrams used to obtain the amplitude of Eq. 3.37.

F.1.3 $hh \rightarrow hh$



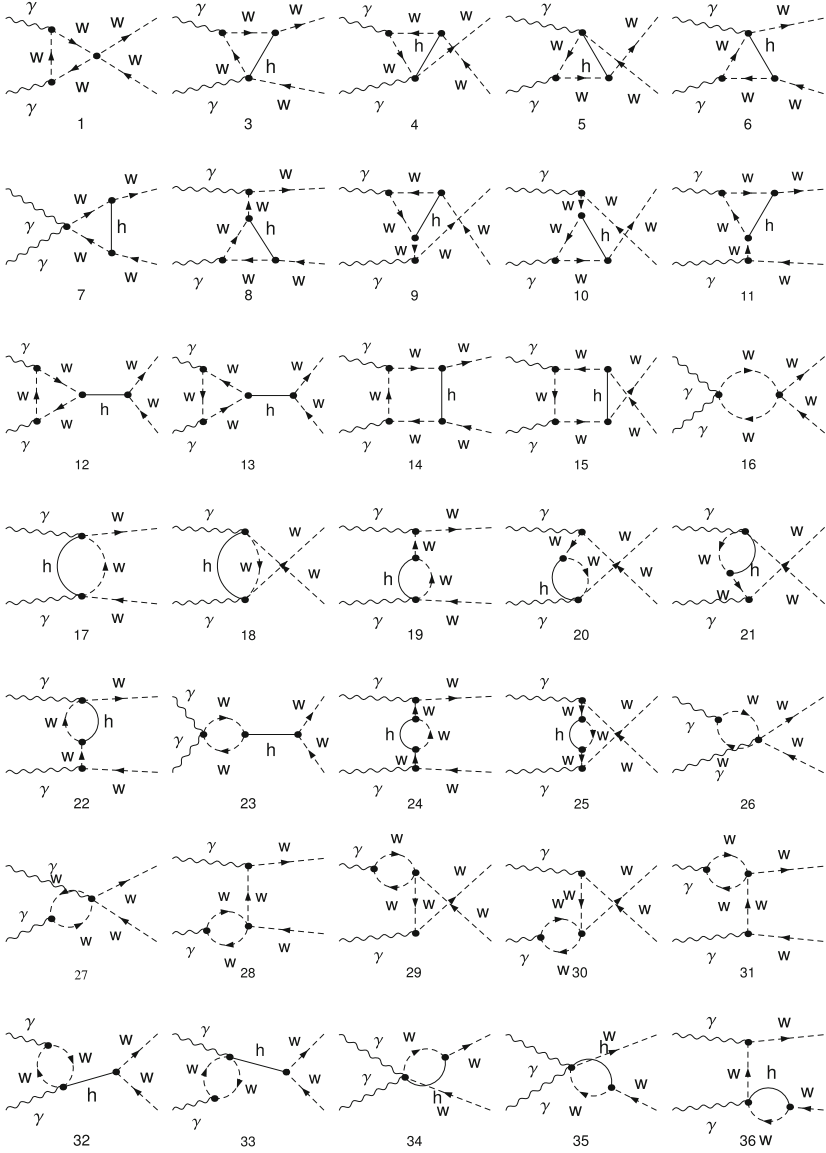
Diagrams used to obtain the amplitude of Eq. 3.41.

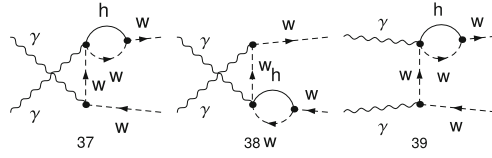
F.2 $\gamma\gamma$ Scattering

Both the spherical and exponential parameterization are used here. See Eqs. 2.33 and 2.34; and Appendices E.3 and E.4 for the Feynman rules. Note the usage of

the charge basis for the description of the ω WBGBs. By definition, the w particle (antiparticle) that appears in the next figures is defined as ω^+ (ω^-).

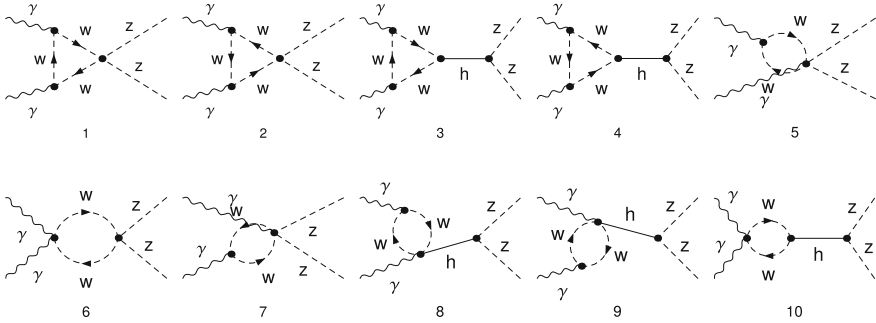
F.2.1 $\gamma\gamma \rightarrow w^+w^-$





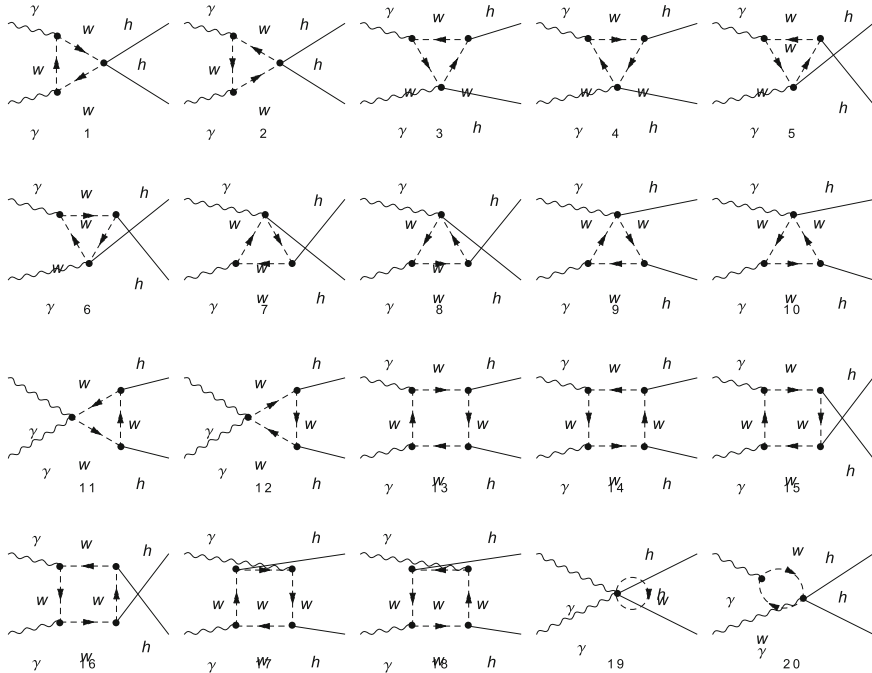
Diagrams used to obtain the amplitude of Eq. 3.57 (Lorentz structure in Eq. 3.51).

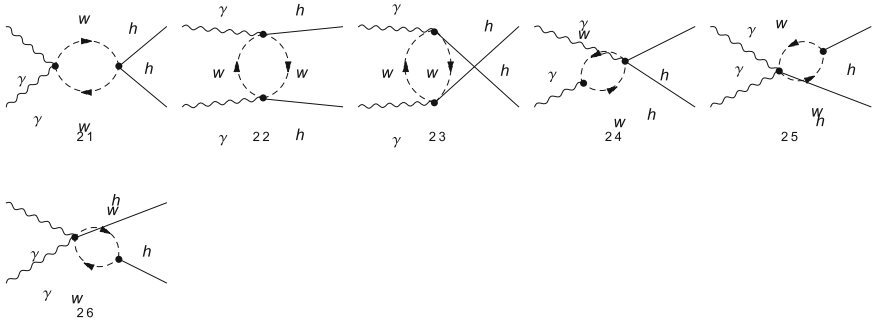
F.2.2 $\gamma\gamma \rightarrow zz$



Diagrams used to obtain the amplitude of Eq. 3.55 (Lorentz struct. in Eq. 3.51).

F.2.3 $\gamma\gamma \rightarrow hh$



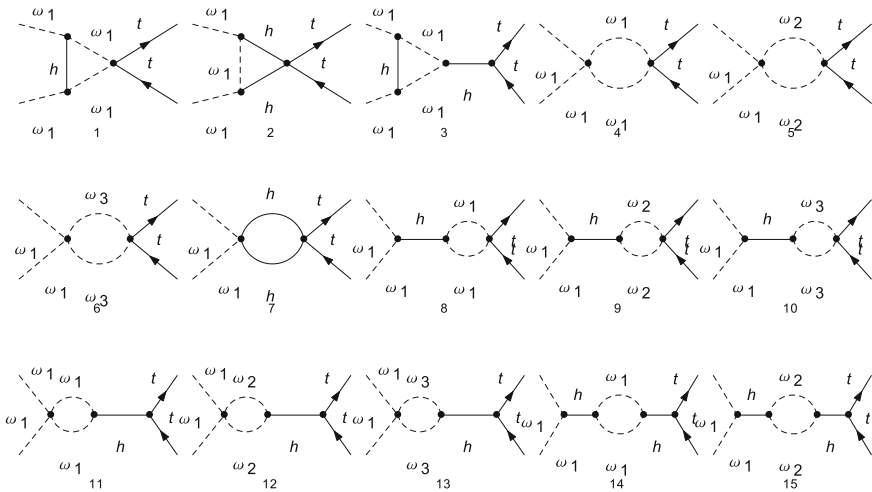


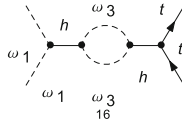
Diagrams used to obtain the amplitude of Eq. 3.87.

F.3 Scattering Involving $t\bar{t}$ States

The exponential parameterization is used here. See Eqs. 2.45 and 2.46 for the considered Lagrangian; and Appendix E.5 for the Feynman rules. Note that we are using the isospin basis, although due to the appearance of terms which break the isospin symmetry we have to consider separately the ω^1 , ω^2 and ω^3 bosons. At the end, all the possible scattering processes $\omega^i \omega^i \rightarrow t\bar{t}$, where $i = 1, 2, 3$, have the same diagrams and matrix element. That is, the isospin symmetry is restored. So, we only paint the diagrams associated with the process $\omega^1 \omega^1 \rightarrow t\bar{t}$.

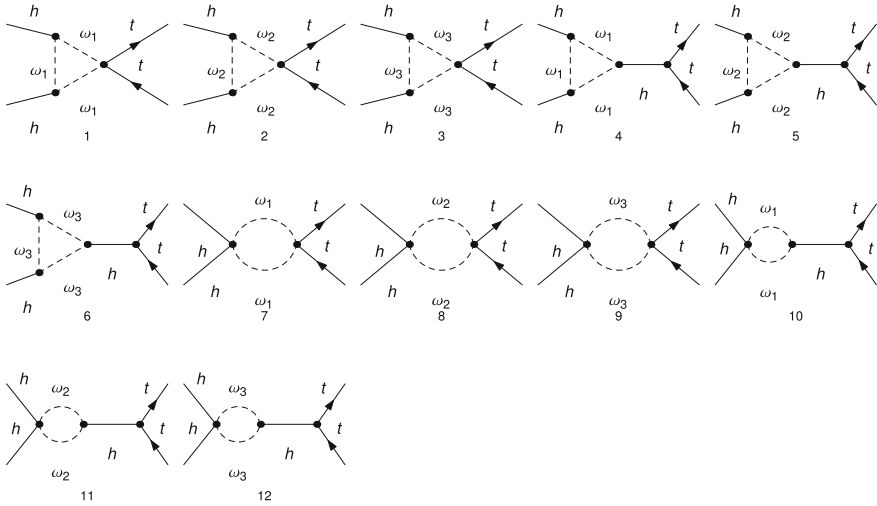
F.3.1 $\omega\omega \rightarrow t\bar{t}$





Diagrams used to obtain the amplitude of Eq. 3.97.

F.3.2 $hh \rightarrow t\bar{t}$



Diagrams used to obtain the amplitude of Eq. 3.108.

References

- 1 T. Hahn, Generating Feynman diagrams and amplitudes with FeynArts 3. Comput. Phys. Commun. **140**, 418–431 (2001)
- 2 A. Alloul, N.D. Christensen, C. Degrande, C. Duhr, B. Fuks, FeynRules 2.0 - A complete toolbox for tree-level phenomenology. Comput. Phys. Commun. **185**, 2250–2300 (2014)
- 3 T. Hahn, M. Perez-Victoria, Automatized one loop calculations in four-dimensions and D-dimensions. Comput. Phys. Commun. **118**, 153–165 (1999)
- 4 J.A.M. Vermaseren, New features of FORM (2000), arXiv:math-ph/0010025 [math-ph]

Curriculum Vitae and Publication List

Dr. Rafael L. Delgado (born in 1989) received his Ph.D. degree on June 2016, with his doctoral dissertation at the Complutense University of Madrid (UCM, Spain). A few months after that, he obtained his habilitation as Assistant Professor from the ANECA (National Agency for Quality Assessment and Accreditation of Spain). He completed his doctoral training with short research stays at the University of Southampton (UK), Max Planck Institut für Physik (Munich, Germany) and the Stanford Linear Acceleration Center (SLAC, Menlo Park, USA).

During his PhD work, he has collaborated with Profs. María José Herrero Solans and Juan José Sanz-Cillero from the IFT-UAM,⁹ and with Prof. Domènec Espriu from the Universitat de Barcelona. During his short stays, he collaborated with Prof. Stefano Moretti (Univ. Southampton), Thomas Hahn (MPI in Munich) and Stanley Brodsky (SLAC). Among his peers, he has worked with Dr. Andrés Fernando Castillo (from the UNAL, Colombia) while his short doctoral stays at the UCM.

The research activity performed in this thesis has lead to a contribution to the CERN's Yellow Report 4 of the LHCHSWG,¹⁰ and to the peer-reviewed articles listed below:

- [1] Andrés Castillo, Rafael L. Delgado, Antonio Dobado, Felipe J. Llanes-Estrada, *Top-antitop production from $W_L^+ W_L^-$ and $Z_L Z_L$ scattering under a strongly-interacting symmetry-breaking sector*,
e-Print: arXiv:1607.01158 [hep-ph], accepted for publication in European Physical Journal C.
- [2] Rafael L. Delgado, Antonio Dobado, and Felipe J. Llanes-Estrada, *Coupling WW , ZZ unitarized amplitudes to $\gamma\gamma$ in the TeV region*,
Eur. Phys. J. C 77, no.4, 205 (2017).
- [3] Rafael L. Delgado, Antonio Dobado, and Felipe J. Llanes-Estrada, *Possible New Resonance from $W_L W_L - hh$ Interchannel Coupling*,
Phys. Rev. Lett. 114, 221803 (2015).

⁹Prof. J.J. Sanz-Cillero has recently joined the UCM faculty.

¹⁰The Yellow Report 4 can be found in <https://inspirehep.net/record/1494411>.

- [4] Rafael L. Delgado, Antonio Dobado and Felipe J. Llanes-Estrada,
Strongly Interacting Electroweak Symmetry Breaking Sector with a Higgs-like light scalar,
Phys. Rev. D **91**, 075017 (2015).
- [5] R.L. Delgado, A. Dobado, M.J. Herrero and J.J. Sanz-Cillero,
One-loop $\gamma\gamma \rightarrow W_L^+ W_L^-$ and $\gamma\gamma \rightarrow Z_L Z_L$ from the Electroweak Chiral Lagrangian with a light Higgs-like scalar,
JHEP **1407**, 149 (2014).
- [6] Rafael L. Delgado, Antonio Dobado and Felipe J. Llanes-Estrada,
One-loop $W_L W_L$ and $Z_L Z_L$ scattering from the electroweak Chiral Lagrangian with a light Higgs-like scalar,
JHEP **1402**, 121 (2014).
- [7] Rafael L. Delgado, Antonio Dobado and Felipe J. Llanes-Estrada,
Light ‘Higgs’, yet strong interactions,
J. Phys. G **41**, 025002 (2014), chosen as one of the Journal’s highlights of 2014.
- [8] Jose A. R. Cembranos, Rafael L. Delgado and Antonio Dobado,
Brane-Worlds at the LHC: Branons and KK-gravitons,
Phys. Rev. D **88**, 075021 (2013).
- [9] Rafael L. Delgado, Carlos Hidalgo-Duque and Felipe J. Llanes-Estrada,
To What Extent is Gluon Confinement an Empirical Fact?,
Few Body Syst. **54**, 1705-1717 (2013).

Additionally, the following contributions to conference proceedings have been prepared. There is also unpublished work in Chaps. 3 and 4 that will be sent in some form.

- [10] Rafael L. Delgado,
Coupling of $t\bar{t}$ and $\gamma\gamma$ with a strongly interacting Electroweak Symmetry Breaking Sector,
Proceedings of the 12th Conference on Quark Confinement and the Hadron Spectrum, (Thessaloniki, Greece, 28/08 - 04/09, 2016),
EPJ Web Conf. **137** (2017) 10001.
- [11] Antonio Dobado, Rafael L. Delgado, Felipe J. Llanes-Estrada, Domenec Espriu,
Comparing mesons and $W_L W_L$ TeV-resonances,
Proceedings of the Bled miniworkshop *Exploring hadron resonances*, (Bled, Slovenia, July 5-11, 2015),
Bled Workshops Phys. **16** (2015), n° 1, 20-26.
- [12] Antonio Dobado, Rafael L. Delgado, Felipe J. Llanes-Estrada,
Resonances in $W_L W_L$, $Z_L Z_L$ and hh scattering from dispersive analysis of the non-linear Electroweak+Higgs Effective Theory,
Proceedings of The European Physical Society Conference on High Energy Physics, (Vienna, Austria, July 22-29, 2015),
PoS EPS-HEP2015 (2015) 173.

- [13] Felipe J. Llanes-Estrada, Antonio Dobado, Rafael L. Delgado,
Describing 2-TeV scale $W_L W_L$ resonances with Unitarized Effective Theory,
Proceedings of the XVIIIth workshop *What comes Beyond the Standard Model?*, (Bled, Slovenia, July 11-19, 2015),
Bled Workshops Phys. 16 (2015), n° 2, 78-86.
- [14] Rafael L. Delgado, Antonio Dobado and Felipe J. Llanes-Estrada,
A Strongly Interacting Electroweak Symmetry Breaking Sector with a Higgs-like light scalar,
Proceedings of the XIth Quark Confinement and the Hadron Spectrum, (Saint-Petersburg, Russia, September 8-12, 2014),
AIP Conf.Proc. 1701 (2016) 090003.
- [15] R.L. Delgado, A. Dobado, M.J. Herrero and J.J. Sanz-Cillero,
Electroweak chiral Lagrangian with a light Higgs and $\gamma\gamma \rightarrow Z_L Z_L, W_L^+ W_L^-$ scattering at one loop,
Proceedings of the 37th International Conference on High Energy Physics (ICHEP 2014), (Valencia, Spain, July 2-9, 2014),
Nucl.Part.Phys.Proc. 273-275 (2016) 703-709.
- [16] Rafael L. Delgado, Antonio Dobado and Felipe J. Llanes-Estrada,
Strongly interacting $W_L W_L, Z_L Z_L$ and hh from unitarized one-loop computations,
Proceedings of the 37th International Conference on High Energy Physics (ICHEP 2014) (Valencia, Spain, July 2-9, 2014),
Nucl.Part.Phys.Proc. 273-275 (2016) 2436-2438.
- [17] R.L. Delgado, A. Dobado, M.J. Herrero and J.J. Sanz-Cillero,
Electroweak Chiral Lagrangians and $\gamma\gamma \rightarrow Z_L Z_L, W_L^+ W_L^-$ at One Loop,
proceedings of the Second Annual Conference on Large Hadron Collider Physics - LCHP 2014, Columbia University (New York, U.S.A, June 2-7, 2014),
arXiv:1409.3983 [hep-ph],
<http://www.slac.stanford.edu/econf/C140602.2/>.
- [18] Antonio Dobado, Rafael L. Delgado and Felipe J. Llanes-Estrada,
Strongly Interacting Electroweak Symmetry Breaking Sector with a Higgs-like light scalar,
delivered at the II Russian-Spanish Congress *Particle and Nuclear Physics at all Scales and Cosmology*, Institute of Cosmos Sciences (Saint-Petersburg, Russia, October 1-4, 2013),
AIP Conf. Proc. 1606, 151-158 (2014).

Finally, there is another article unrelated with the topic of this PhD thesis,

- [19] R.L. Delgado, P. Bargueño, F. Sols,
Two-step condensation of the charged Bose gas,
Phys. Rev. E 86 (2012) 031102.